On the Properties of a Few Electron-Hole system in a Double One-dimensional Harmonic Trap

Fan Pan

Supervisors:

Prof. Stephanie M.Reimann

Lìney Halla Kristinsdóttir

October 21, 2012

Abstract

In solid state physics, the combination of an electron and a positively charged hole (absence of electron) is known to play a very important role. Such a combination is called an exciton. It is electrically neutral and can move around and transfer energy like a particle.

Excitons are experimentally studied in several branches of physics, such as when dealing with optical lattices, quantum dots and nano-materials. However, such studies have primarily focused on a large number of excitons. The study of a system of a few excitons is still a challenging task for experimentalists.

It would be of great interest to present a theoretical study of some aspects of a few-exciton like system, through analytic calculations as well as numerical simulations. Results thus obtained could be relevant to future experimental work. However, this task being difficult it makes sense to start with a simpler model. Therefore, in this project I will focus on the ground state of a few exciton system, where the electrons and the holes are in separate one dimensional (1D) harmonic traps. Using configuration interaction method I obtain numerical results. It is found that, in obtaining the energy spectrum as well as density localization and fermionization, the key parameters are the separation of the traps and the strength of the interaction.

I present a comparison of a variety of 1D models, including cases where fermions are replaced by bosons. In this case, short-range contact interactions are used instead of Coulomb interactions. Also, to further understand this system, some bonus has got from dipolar interactions.

Contents

List of Figures

Chapter 1

Introduction

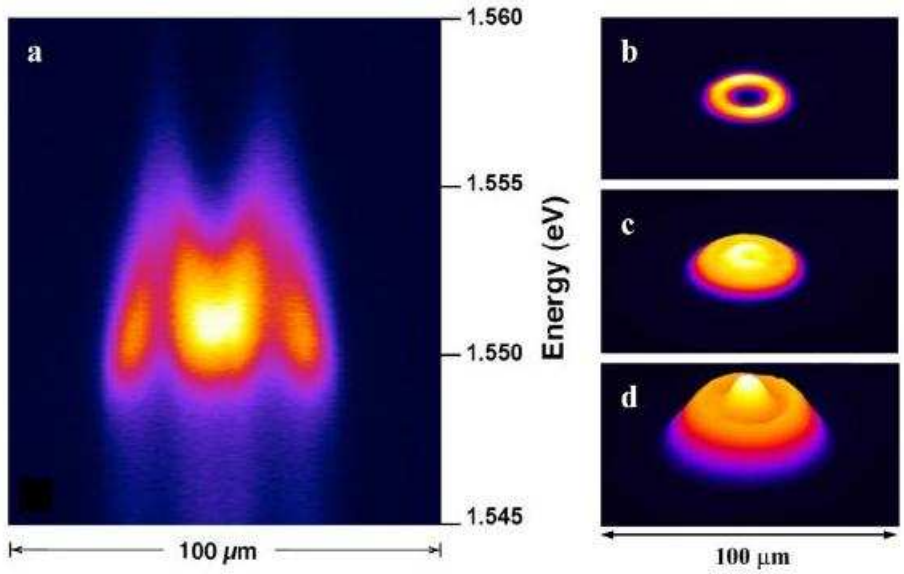

Figure 1.1: (taken from Ref. [18])
Images of laser-induced trapping of excitons.

My work, presented in this thesis, has been inspired by excitons.

One of the most important concepts in condensed matter physics is that of "quasi particles". The exciton is one such quasi particle. In semi-conductors, excitons are formed by the excitation of electrons from valence band to conduction band, which creates holes in the valence band. Because of the Coulomb force, the electron and the hole are attracted to each other and can form a "hydrogen-like" bound state called the exciton.

The physics of excitons is quite subtle. Here I only would like to mention that there are two major classes of excitons: the Frankel exciton and the Wannier-Mott exciton.

In the Frenkel model, from 1931 [1] the Coulomb interaction between the electron and the hole is taken to be relatively strong. This happens in materials with small dielectric constant. The electron and the hole are then tightly bound to each other and form a "hydrogen-like" atom, with a small Bohr radius. This exciton is rather sharply localized, its wave function hardly extends beyond the unit cell. The binding energy of this kind of exciton is typically of the order of 0.1 to 1 eV. Frenkel's original motivation for proposing the exciton was to introduce a new mechanism for transfer of energy in materials. His point was that excitons being neutral can move freely and transport energy to rather large distances inside a material while electrons tend to collide and scatter and thus have harder time to travel inside the material.

Frenkel's seminal idea had a great impact and led to invention of other types of excitons. A notable one among them was proposed [2] in 1937 by and nowadays goes under the name of Wannier-Mott exciton. In this case one considers materials with relatively large dielectric constant. The Coulomb interaction between the electron and the hole is screened, giving rise to a more weakly bound system. This type of exciton has typically a binding energy of about 0.01 eV and a size (wave function) that extends over several unit cells.

One notable property of excitons is that they are composite bosons. Bosons are known to form condensates, as was predicted already in mid 1920's (Bose-Einstein condensation, BEC). Such condensates manifest themselves in phenomena such as superfluidity and superconductivity. A question which has often been raised in the literature is: do excitations form condensates [3]?

The issue of exciton condensate is more relevant today than ever before because a great deal of progress has been made in experimental techniques for producing condensates. Since 1995 one has been able to produce condensates of several different kinds of atoms, such as Rb, Na, Cs, Ca, and even hydrogen [19, 20, 21]. These methods give a new hope for a more successful production and study of exciton condensates.

One major problem with excitons is their short lifetimes while in order to be able to detect and study their condensates their lifetime should preferably be longer than the cooling time. The electron and the hole tend to recombine and emit light. For recent experiments focus on semiconductor structures with two coupled parallel quantum wells, see [4]. One distinguishes between two types of excitons:

type A and type B. Type A excitons are produced via applying a magnetic field and type B by primarily employing an electric field. The experimentalists have great expectations that the type B excitons (also referred to as "spatially indirect" or simply "indirect" excitons) will be very useful for future research. The point is that these type B excitons can be made to have much longer lifetimes by increasing the strength of the applied electric field.

I would like to add that excitons have been investigated in many different materials, for example the single-walled carbon nanotubes, semiconductor quantum dots and organic polymers. One branch of these studies concerns solar cells. Since the excitons play an important role in converting photonic energy to electronic energy as well as for transport of energy, some researchers are trying to find high efficiency "exciton-friendly" materials that would be suitable to use in solar cells.

Excitons are undoubtedly exciting objects but in general too complicated to deal with in detail. Instead, the purpose of my work has been to investigate some of the fundamental properties of a few oppositly charged particles placed in a one-dimensional (1D) bilayer harmonic trap. The topology of the system I consider looks similar to that of type B exciton [4]. In order to get started and make some progress I have had to make a number of simplifying assumptions. The most important assumption is that the opposite charged particles do not recombine, i.e., the lifetime of the corresponding excitons is infinitely long. Furthermore, I have taken the interaction between the particles to be Coulombic and have neglected the exchange contribution as well as the effects due to spin.

The plan of the this thesis is the following:

The model that I have used is introduced in Chap. 2. In Chap. 3 I point out the advantage of configuration interaction (CI) methods and give some details of technical issues related to programming. In Chap. 4, I present the numerical results for four models. These are: the double 1D trap with fermions (section 4.1), the single 1D trap (section 4.2), the double 1D trap with bosons (section 4.3), and 1D ideal-dipole model (section 4.4). Finally, Chap. 5 summarizes the conclusions of my work and presents the outlook.

Chapter 2

Description of the model and its parameters

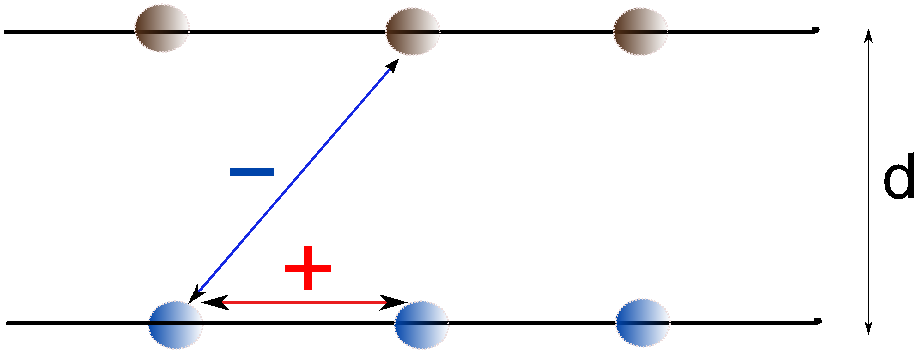

Figure 2.1: A schematic diagram of the system under study in the case of Coulombic interaction. Particles sit in two thin cigar-shaped traps. Equal numbers of electrons and holes reside in each trap. The plus (minus) sign indicates that the interaction is repulsive (attractive).

We consider several interacting charged particles in a double one-dimensional(1D) harmonic trap. Ignoring the spin degrees of freedom, these particles can either be spinless bosons or polarized spin-1/2 fermions (with the same spin orientation). The many-particle Hamiltonian for such a system is (Fig. 2.1),

$$\hat{H} = \hat{H}_{kin} + \hat{H}_{ext} + \hat{V}_{int} \tag{2.1}$$

where $\hat{H}_{kin}$ and $\hat{H}_{ext}$ both are one-body harmonic oscillator operators, labeled as

the kinetic part and external confinement, respectively

$$\hat{H}_{kin} + \hat{H}_{ext} = \sum_{i=1}^{n} \left(\frac{\hat{p}_i^2}{2m} + \frac{1}{2} m\omega^2 x_i^2 \right) \tag{2.2}$$

Here x_i (P_i) denotes the position (momentum), m is the mass and ω the angular frequency.

The interaction term $\hat{V}_{int}$ arises from both attractive and repulsive Coulomb forces [5].

$$\hat{V}_{int} = (-1)^{a_{ij}} \frac{1}{2} \sum_{i \neq j}^{n} \frac{e^2}{4\pi\varepsilon_0} \frac{1}{\sqrt{|x_i - x_j|^2 + a_{ij} d^2}} \tag{2.3}$$

where ε_0 is the electrical permittivity. The parameter a_{ij} is defined by:

$$a_{ij} = \begin{cases} 0 & \text{if particles } i \text{ and } j \text{ are in the same trap} \\ 1 & \text{if in different traps} \end{cases}$$

The interactions between particles, as seen from Eqs. 2.3 depend on the relative distance

$$x_{ij} \equiv |x_i - x_j|$$

between them. Therefore the sum in Eqs. 2.3 contains $n(n-1)/2$ terms.

Although written as one-dimensional, in fact the true confinement should be first evaluated in three-dimensions

$$\hat{H}_{ext} = \sum_{i=1}^{n} \frac{1}{2} m \left(\omega^2 x_i^2 + \omega_\perp^2 (y_i^2 + z_i^2) \right) \tag{2.4}$$

which allows the one-dimensional trap to be elongated in the x direction and be transverse symmetric in y and z. Here there are two important length scales. The first one is

$$l = \sqrt{\hbar / m\omega} \tag{2.5}$$

associated with the longitudinal trap ("X-trap") and the second one, the transverse length scale

$$l_\perp = \sqrt{\hbar / m\omega_\perp} \tag{2.6}$$

We introduce the parameter λ

$$\lambda = \frac{l_\perp}{l} \tag{2.7}$$

This specifies the asymmetry of the external confinement: for $\lambda \gg 1$ the trap is disk-shaped; while for $\lambda \ll 1$ the trap is cigar-shaped. In our case, setting $\lambda \ll 1$ [1] (or $\omega_\perp \gg \omega$) gives rise to the quasi one-dimensional geometry.

To see how λ enters into the picture, one can consider the quantized energy levels, simply written as

$$\epsilon(n_x, n_\perp) = \hbar\omega(n_x + 1/2) + \hbar\omega_\perp(n_\perp + 1) \tag{2.8}$$

where n_x and $n_\perp$ are harmonic oscillator quantum numbers.

Since $\omega_\perp \gg \omega$, by changing the quantum number $n_\perp$ from 0 to 1 the contribution to Eqs. 2.8 is much larger than the level spacing fixed by $\hbar\omega$. In this sense, we may fix the transverse degrees of freedom to the ground state, which means neglecting the energy contributed from $\hbar\omega_\perp(n_\perp + 1)$. Thereby the original expression (Eqs. 2.2) is obtained.

To further simplify the calculations, we define the energy in unit of $\hbar\omega$, associated with

$$l = \sqrt{\hbar/m\omega}$$

and put

$$x = \xi \cdot l$$

where ξ is a dimensionless number. The Hamiltonian now has the form :

$$\hat{H} = \hat{H}_{kin} + \hat{H}_{ext} + \hat{V}_{int} \tag{2.9}$$

$$= \sum_{i=1}^{n} \Big(\frac{-\hbar^2}{2ml^2} \frac{\partial^2}{\partial \xi_i^2} + \frac{1}{2} m\omega^2 l^2 \xi_i^2 \Big) + (-1)^{a_{ij}} \sum_{k=1}^{\nu} \frac{e^2}{4\pi\varepsilon_0 l} \frac{1}{\sqrt{\xi_k^2 + a_{ij}(d/l)^2}} \tag{2.10}$$

$$= \hbar\omega \Big[\sum_{i=1}^{n} \Big(-\frac{1}{2} \frac{\partial^2}{\partial \xi_i^2} + \frac{1}{2} \xi_i^2 \Big) + (-1)^{a_{ij}} \sum_{k=1}^{\nu} \frac{e^2 ml}{4\pi\varepsilon_0 \hbar^2} \frac{1}{\sqrt{\xi_k^2 + a_{ij}(d/l)^2}} \Big] \tag{2.11}$$

Another variable of interest is the interaction strength, also called the factor g

$$g = e^2 ml / 4\pi\varepsilon_0 \hbar^2 \tag{2.12}$$

which is the pre-factor of Coulombic interaction. It shows that increasing the particle's effective mass or charges will modify the strength of interaction term. This factor g will be studied thoroughly in chap. 4. Note again that the positive and negative values of $(-1)^{a_{ij}}$ correspond to effective repulsion and attraction between the particles, respectively.

[1] λ is typically of the order of 0.1 to 0.01.

Another interesting variable is the separation d of the two traps. Modifying d will directly change the attractive forces, while it has no direct effect for the repulsive. However in a coherent system, the separation between particles will affect the density of the particles as distribution has been mapped by the attractive forces. Therefore the separation will affect the repulsive forces indirectly. It is also worth to note that by comparing the double 1D trap with the single 1D trap, the attractive interaction in double 1D trap decreases very quickly when d becomes larger. To study the double 1D trap we need first to find the proper range of d, and in particular determine the lower limit on d, originating from the convergence problem mentioned before.

Chapter 3

C++ programming and CI library

Road map: In this chapter, our task is to describe the numerical method and its implementation. To begin with, we introduce some basic C++ programming concepts, from which we explain why C++ is commonly seen as object-oriented programming language. In the following we discuss how to use the configuration interaction (CI) library to obtain the numerical results. A corresponding translation has been shown to connect CI method to C++ programming language. Finally we discuss how trustworthy the results are.

3.1 Introduction to the C++ object technology

Classes, Data Members and Member Functions

The best way to understand these concepts is to find some familiar stuff [6]. The Class could be thought of as a blueprint of an object. In related other words, it is a "design" of how to create one kind of product, for example a car "design" or a house "design" corresponding to a 'car Class' and a 'house Class'. Since these "designs"(Classes) provide some 'services' to the clients, the Data Members are used to fulfill the different demands from clients, for example 'the size of a car' or 'the height of a house' etc. Once we create a class, we can have as many objects as needed, which are designed by different parameters. The function components of a class are called Member Functions. These can be thought of as the "building blocks" used for producing the object in question. To construct a car, we need wheels, tyres, windows etc.; these materials in this case represent Member Functions of a Class. In addition, the Member Functions of one class can be reused in another class. For instance, when we build a 'house Class', we can simply borrow the "window" Member Function from a 'car Class'.

Inheritance and Polymorphism

To introduce some key features of the object-oriented programming, we will use the basic C++ concepts that have been mentioned before. One important concept is named "inheritance". It means that the programmer absorbs Data and Member Functions, from an already existing class, into a new class and thus enhances its capabilities. The existing class is called the Base Class, and the new class is referred to as the Derived Class. Note that a Derived Class is a subgroup of a Base Class. The "inheritance" seems to be an "one-way ticket" that can only be used from a Base Class to its Derived Class.

The inheritance can be achieved by several steps. We take the example of an orchestra: the string *is* a component of the orchestra, the violin *is* a component of string, the first violin *is* a component of violin. Therefore, the inheritance relationship from 'orchestra Class' to 'first violin Class' form a tree-like structure, which represents a hierarchy with 4 levels.

Another feature called Polymorphism is closely related to the Inheritance. Polymorphism enables us to program in a general way rather than program in a specific way. We take another example: assume that there are classes 'violin' , 'flute' and 'harp' representing three types of instruments. Each of these classes is inherited from the base class 'instrument', which contains a function 'play'. The different classes respond to the same function 'play' in a different way. This "one" to "many" form is the key point of polymorphism.

The CI library is a collection of classes, which implements the CI methods for different geometry models, `harmonicoscillator 1d`, `harmonicoscillator 2d`, `cylinder 2d`, `ring 1d` etc. The inherited structure is shown in Fig. 3.1, which indicates the inheritance relationship in the real CI library. The basic class in our case is `Harmonic1D`, from which we derive another class `harmonic1D-withRelativeDistance`, which has been specified with an additional condition: the distance used in the interaction term is the relative distance between the particles. Likewise the double 1D class derived from the single 1D class shows similar inheritance pattern. Therefore, the `DoubleHarmonic1DwithRelative-Distance` is a derived class of the base class `Harmonic1D`. In this way, it can directly use the data members and member functions which have been defined in its base class.

To explain the enhanced part, we have to use our knowledge of polymorphism. The double 1D system is more complex than the single 1D system as it includes both repulsive and attractive interactions, while the single 1D systems only have repulsions. Therefore, the member function which provides the interaction terms

has to be changed. Actually, the interaction member function in the base class has been defined as a “virtual” type, without specific function coded but as a spare name only. The polymorphism “one” to “many” is achieved by taking the same routine for each interaction member function which, however, receives different reactions. One can envisage the member function of the interaction term as a “black box”; the base class only puts this black box in the “right place”, which has to be linked to other member functions. Each derived class defines its own interaction term so as to supply the “black box” with details. Therefore, one is free to specify any type of interaction to be investigated under the same geometric model, for example the contact interaction, the Coulomb interaction, etc.

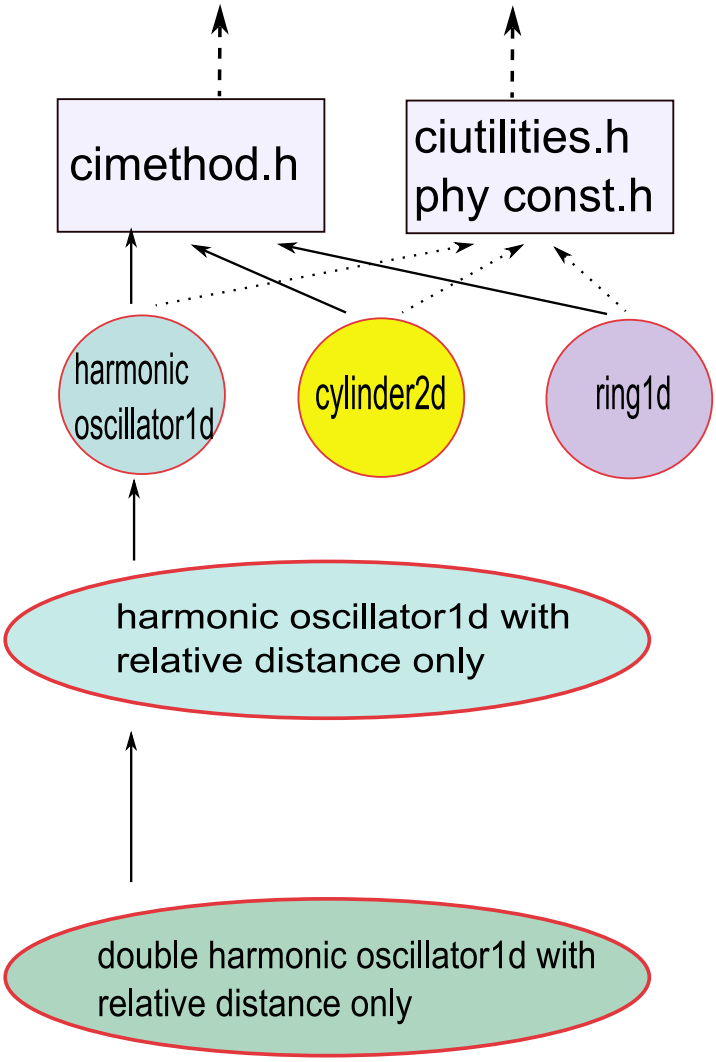

Figure 3.1: Inherited structure of CI library

3.2 Second quantization and CI method

In this part, we will follow the programming logic and translate it into the CI method language. Though it is not the same as found in textbooks about the second quantization and CI method, but it is how it works in reality. Here below, I

present the essential part of my code listing in the right column, and explain how I have implemented them in the corresponding left column. Thus we try to fill the gap between the "theorems" and their numerical implementations [7].

Second quantization formalism	C++ programming by CI library
`spos` is an object generated by the `double_1D` class. This name is obtained from the initial letters 'Single Particle Orbital Set'. To create this object, we need two parameters: the number of orbitals and the number of spins. Thus we generate a string of $\|\phi_i\rangle$: $\|\phi_1\rangle$ $\|\phi_2\rangle$ $\|\phi_3\rangle$, for a spinless particle with 3 single particle orbitals, etc. In addition, the class includes the member functions `OneBodyOperator` and `TwoBodyOperator`, which are composed of creation and annihilation operators: $$\hat{H}^{(1)} = \sum_{i,j=0}^{n} \sum_{s,s'} t_{isjs'} \hat{a}\dagger_{i,s} \hat{a}_{j,s'}$$ $$\hat{H}^{(2)} = \sum_{i,j,k,l=0}^{n} \sum_{s,s',s'',s'''} v_{isjs'ks''ls'''} \hat{a}\dagger_{i,s} \hat{a}\dagger_{j,s'} \hat{a}_{k,s''} \hat{a}_{l,s'''}$$ Here we need to calculate the matrix elements $t_{isjs'}$ and $v_{isjs'ks''ls'''}$. This work is done by another member function `matrixElement`, which supplies a real number value for each overlap integral.	`double_1D spos( Orbitals, Spins, InteractionFunction )`
`basis` is the object of class `ManyBodyBasisSet`. It generates the many-body basis from the single-particle basis for a given number of particles in total. This many-body basis is commonly called a "Fock space" and is denoted by $P^{(N)} = \{\|\Phi_\nu^{(N)}\rangle\}$, where N is the number of particles, and the label ν is the order which has been used in the single-particle orbitals. Note that one has to specify whether the particles are fermions or bosons, where we can see the advantages of using the property of Polymorphism. Taking as an example 3 particles and 3 single particle orbitals, the basis for bosons will result in 10 possible states:	`ManyBodyBasisSet basis( spos, "FERMIONS,N=3" )`

|3 0 0⟩
|0 3 0⟩
|0 0 3⟩
|2 1 0⟩
|2 0 1⟩
|1 2 0⟩
|1 0 2⟩
|0 1 2⟩
|0 2 1⟩
|1 1 1⟩

whereas for fermions, it can only be:
|1 1 1⟩

From the many body basis, there is no difficulty to create an empty matrix which has the same dimensions as the many body basis set denoted as $d_{P^{(n)}} * d_{P^{(n)}}$. This matrix will be used to store the matrix representation for one-body operator $[\hat{H}^{(1)}]$ and two-body operator $[\hat{H}^{(2)}]$.

```
basis.getBasisSize()
```

Since we choose the single particle orbitals as the eigenfunctions of the one-body Hamiltonian, the corresponding matrix representation is already diagonal. The eigenvalues are simply the energies of the individual particles :

$$[\hat{H}^{(1)}] = \begin{bmatrix} \langle\Phi_1|\hat{H}^{(1)}|\Phi_1\rangle & \dots & \\ \vdots & \langle\Phi_2|\hat{H}^{(1)}|\Phi_2\rangle & \dots \\ & \vdots & \ddots \end{bmatrix}$$

However, the $[\hat{H}^{(2)}]$ part is not diagonal, calculating its matrix elements is much more complicated than dealing with $[\hat{H}^{(1)}]$.

The following steps will focus on the CI post-processing methods. The total Hamiltonian is the sum of $[\hat{H}^{(1)}]$ and $[\hat{H}^{(2)}]$,

$$[\hat{H}^{(tot)}] = [\hat{H}^{(1)}] + [\hat{H}^{(2)}]$$

and we have

$$[\hat{H}^{(tot)}]|\Psi\rangle = E|\Psi\rangle$$

`matrix.diagonalize()`

where $\Psi\rangle$ is the real many-body wave function.
This diagonalization can be carried out, from which we will obtain the corresponding ground state energy and wave function.

In order to visualize the many-particle wavefunction, firstly we can evaluate the single-particle density distribution at any position x. This quantity is defined by:

$$\rho^{(1)}(x) = \langle\hat{\Psi}^{\dagger}(x)\hat{\Psi}(x)\rangle = \sum_{i,j} \phi_i^*(x)\phi_j(x)\langle\Psi^{(N)}|\hat{a}_i^{\dagger}\hat{a}_j|\Psi^{(N)}\rangle$$

`calculateDensity1D`

We could also place one of the particles at the reference position x' and calculate the pair density distribution for the remaining $N-1$ particles :

$$\begin{aligned}\rho^{(2)}(x,x') &= \langle\hat{\Psi}^{\dagger}(x)\hat{\Psi}^{\dagger}(x')\hat{\Psi}(x')\hat{\Psi}(x)\rangle \\ &= \sum_{i,j,k,l} \phi_i^*(x)\phi_j^*(x')\phi_k(x)\phi_l(x')\langle\Psi^{(N)}|\hat{a}_i^{\dagger}\hat{a}_j^{\dagger}\hat{a}_l\hat{a}_k|\Psi^{(N)}\rangle\end{aligned}$$

`calculatePair-CorrelateDensity1D`

where the reference position x' should be chosen at a high density that $\rho^{(1)}(x)$ is large.

The occupation number (ratio) presents how many single particle orbitals have been used to construct the many body wavefunction. It provides a way to check if we have included a large enough number of orbitals.

`calculateOccupation-Numbers`

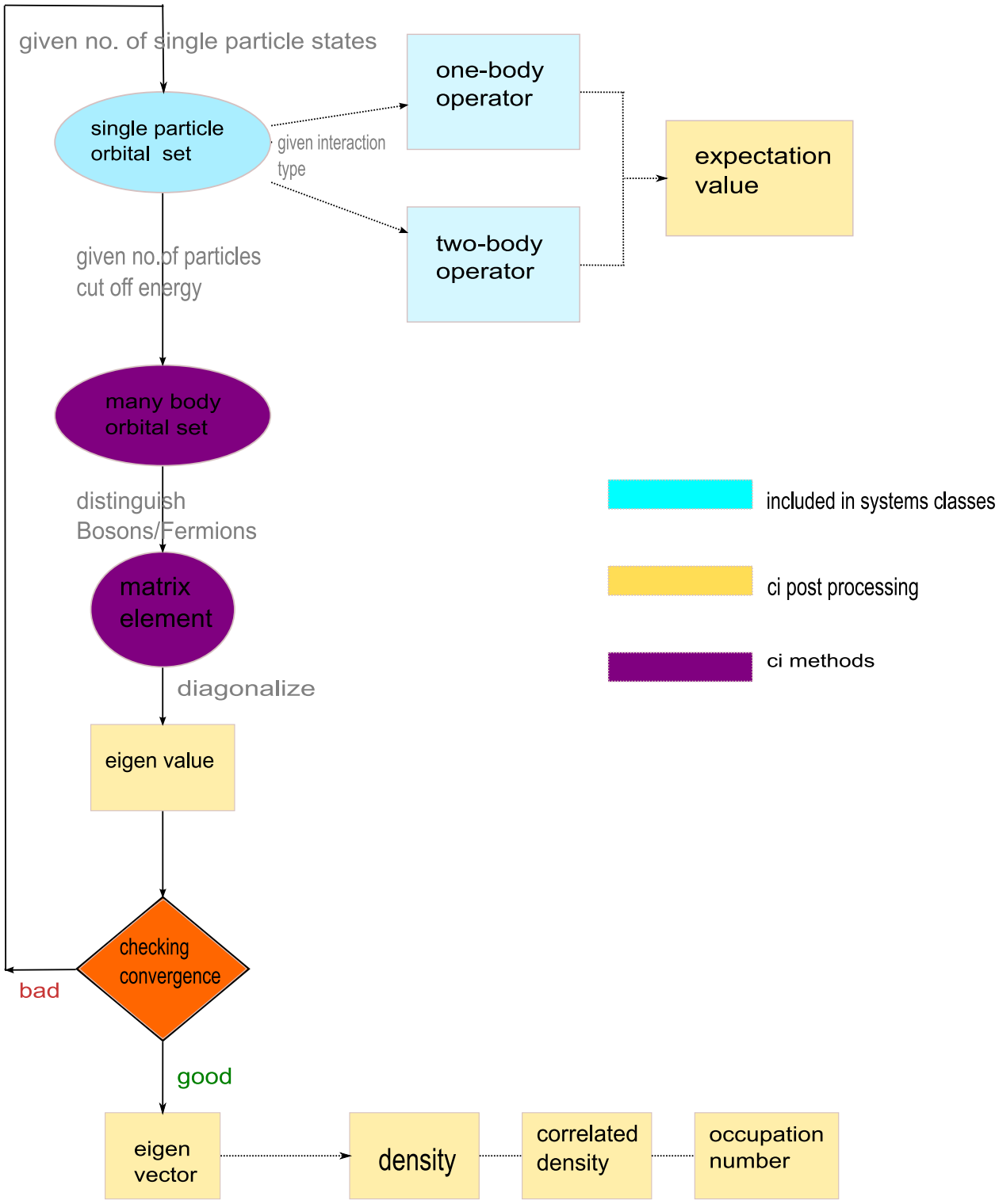

Figure 3.2: Simplified programming flow sketch.

3.3 Convergence issue

The convergence is the major problem that we need to worry about. It is highly related to how much we can trust the results. This problem will also put strong limits on the range of parameters. For example consider the issue of time needed to do the computations. We can not enter the region for the double trap with extremely small separation or with very large interaction strength. In this section, we will discuss methods for examining the convergence issue via energy profiles and occupation ratio profiles.

3.3.1 Hilbert space cutoff

There are two ways to determine the size of Hilbert space in our numerical method: the energy-cutoff and the single-particle-orbital-cutoff. No matter which method is applied, a larger basis gives a greater accuracy. It has been shown that taking a larger number of single particle orbitals leads to a lower value of energy. Note that the results obtained via CI method is the upper bound of the true value. This point can be seen from the energy profile (Fig. 3.3). However, firstly we should discuss why we choose single-particle-orbital-cutoff in our case. As the single particle orbitals are chosen for the eigenstates of single particle operators, the matrix representation of Hamiltonian neglecting interactions is diagonal. The cutoff energy in this case only depends on this part of energy. Therefore, this method can be used if we know that the interaction energy is much smaller than the kinetic plus the potential energy. This happens in most cases, in which the interaction term can be treated as perturbation. However in our model the interaction strength g is allowed to vary over a wide range. Therefore, we don't know whether the interaction energy is only a perturbation added in the system, which would make it safe to use single-particle-orbital-cutoff method.

Since the results should be independent of the truncation scheme; a good convergence would imply that the energy can not be further reduced by continuing enlarging the basis. On the other hand, if we know the smallest number of orbitals needed to get convergence in each case, we can just use the minimum number of orbitals for different cases in order to save computation time.

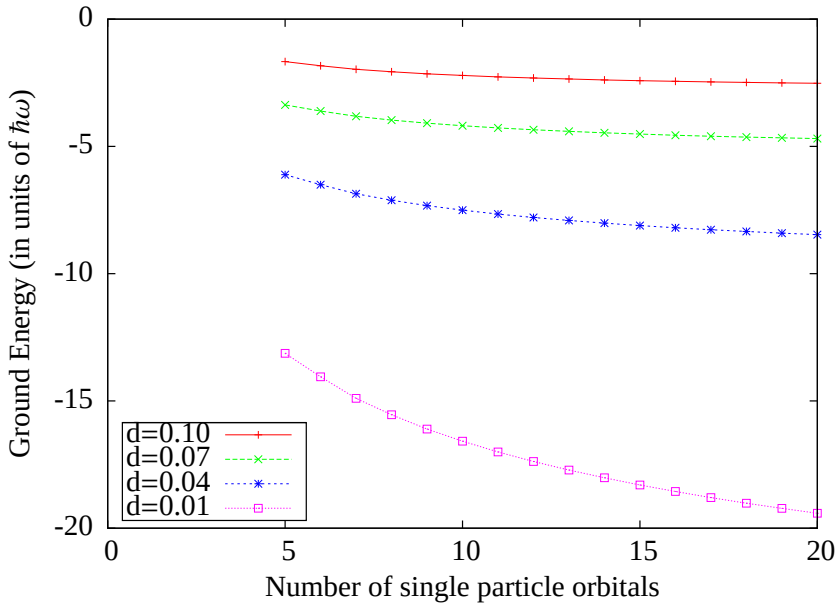

Figure 3.3: Examining the convergence for the case of $N = 6$ fermions and $g = 1$.

The worst scenario for convergence shown in Fig. 3.3 is for $d = 0.01$. It implies that even using the single particle orbitals up to 20, is not enough for distance of about 0.01. In this case, the 20 single particle orbitals will create roughly 10^6 particle states which means that the Hamiltonian will be represented by a 10^6 by 10^6 matrix. The required computer running time would be around hundred hours! The convergence problem changes by varying the parameters d and factor g. It also depends on the statistics used; the case for bosons is even more difficult than for fermions.

3.3.2 Occupation numbers

Another way to investigate the size of a basis and the set of many-body states is through the occupation ratio profiles (Fig. 3.4). The figure shows the fraction of individual single particle orbitals used in the composed many-body states. In this case, we compare the results by varying two parameters: the interaction strength g and the separation distance d.

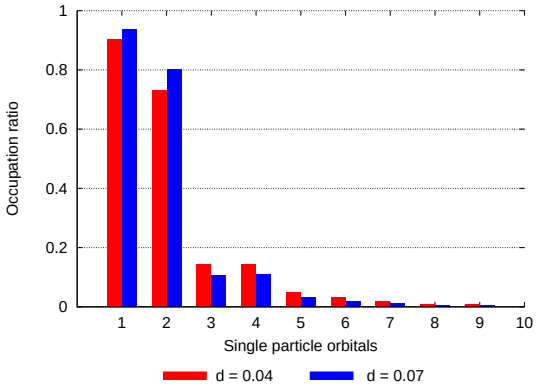

(a) $g = 1.0$

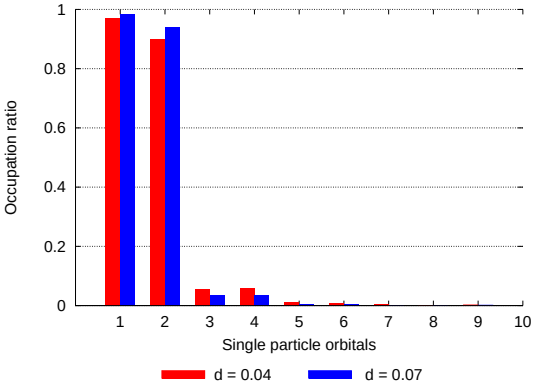

(b) $g = 0.6$

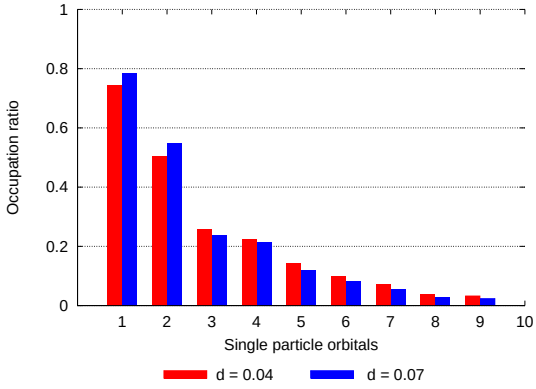

(c) $g = 2.0$

Figure 3.4: The occupation number n_i for 2 fermions in the Fock space.

In each of the cases, the occupation ratio has been normalized. In this case, we put 2 particles in each trap, the sum of occupation numbers for all the single orbitals is 2. It can be generalized as $\sum_i n_i = N$.

For $g = 1$, the occupation ratio of the lowest two orbitals are shown to be much higher than other orbitals. This point shows more clearly by using a smaller value of g, as we can see that the ratio for higher orbitals almost drops to zero (Fig. 3.4b). By contrast, more higher orbitals are used in the case of larger g (Fig. 3.4c). The parameter d can also affect the occupation ratio but in a minor sense. Comparing the profile with the same interaction strength g but different d, we see that the case of smaller d would need to use more higher orbitals than the case of larger d. It implies that the convergence issue must be paid more attention

to as we explore a system which is parametrized by a larger factor g or a smaller d. In both cases the reason is that the lower single particle orbitals couple to a larger number of higher orbitals.

In conclusion, in this chapter we have first introduced some basic ideas of C++ programming, then focused on the implementation of CI method in a practical way. Finally, we have emphasized the importance of the convergence issue and the limitation of CI method. To begin with some numerical results related to the convergence issue have been shown. Further results will be discussed in the next chapter.

Chapter 4

Results and Discussion

Road map: In this chapter, we first display the results for the double one dimensional (1D) trap with fermions. The double 1D trap can be seen as composed of two single 1D traps. A comparison between a double 1D trap and a single 1D trap has been made. Since the fermions and bosons obey different statistical rules, in analogy with fermions, the same procedure has been investigated for bosons with double 1D trap. For each system, we will focus on its energy plots and the density distributions. Moreover, the double 1D trap with electrons and holes can be viewed as a 1D trap with dipoles. A qualitative comparison between these two systems will be given at the end of this chapter.

4.1 Double 1D trap with fermions

4.1.1 The energy of the ground state

The CI method is well suited for investigating few body systems. We have chosen the case of three electrons or holes in each trap, respectively. The Hamiltonian of the system can be parametrized by the distance d and the interaction strength factor g. We investigate the sensitivity of our results to the changes in these parameters in two ways: we fix the factor g and change d in a certain range (Fig. 4.1a), or in an alternative way fix d and change g (Fig. 4.1b). In the first case, setting d in the range of 0.2 to 2 has multiple reasons, d not only has been limited by the convergence issue as we mentioned before, but also has to fit the condition of quasi 1D geometric by yielding $d \gg l_\perp$, where $l_\perp$ is the radial oscillator length.

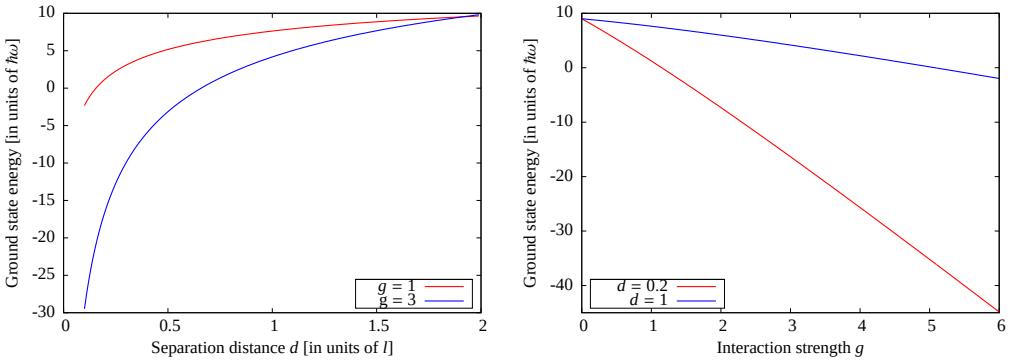

(a) fixed g,varying d (b) fixed d,varying g

Figure 4.1: Ground state energy for $N = 6$ fermions in a double 1D trap.

For a double trap, the energy of the ground state starts to increase as the distance d becomes larger, because d strongly affects the attractive Coulomb forces which can decrease the total energy. As d becomes large enough, the attractive forces can only play a minor role. Not surprisingly the energy tends to saturate for both cases. Furthermore, the curve for $g = 3$ has a higher increasing ratio and lies below the curve $g = 1$, before a crossing at around $d = 2$ (Fig. 4.1a). We note that varying range for d up to 2 is reasonable, since beyond this range, the double trap can be approximately seen as two isolated single traps, in which we are not interested at the moment (further arguments will be presented in the 1D single trap discussions).

The interaction term affecting the energy is shown in Fig. 4.1b. The data are shown from $g = 0$, since at this point, there are no interactions for both cases. After we "switch on" interactions, the attractive interaction will compete with the repulsive ones and reduce the energy almost linearly as g increases. The energy drops more quickly for $d = 0.2$ than $d = 1$.

4.1.2 The density distribution

For the density profiles, we will discuss the case that three electrons or holes are contained in each trap. The range for parameters d and g is taken to be the one we already used in the energy plots. In this sense, from the density profiles, one can see the system optimizing its total energy in each case. This can be done by mapping its particles into different configurations. When we display the results, we only need to show either electrons' or holes' distribution, because the

distribution for both are equivalent, so it is unnecessary to specify which kind of particles is involved.

The definition of the g factor has been given before (Eqs. 2.12). It is proportional to the effective mass m, the harmonic oscillator length l, the square of the effective charge e^2 and one over permittivity $1/\varepsilon_0$. The physical interpretation of different g can be understood by taking particles with different effective mass and charge or different materials, while the value of l has been fixed. Although for a harmonic confinement, tuning the oscillator length l is a general way to control the system from experimental point of view, here we have to fix l in order to be able to compare the results for all the cases. Note that l is used as the length unit for the coordinates, in the same sense as $\hbar\omega$ is used as the energy unit. Thus, we can be confident that the scale of their units does not change in any of the cases that we have studied.

Note that as a functiion of the relative distance applied here, the distribution is always central symmetry. Besides each particle roughly occupies the width of about one unit in spatial space, which allows us to fit the whole profile in the width of 8 units (the reason of X-relative being from -4 to 4).

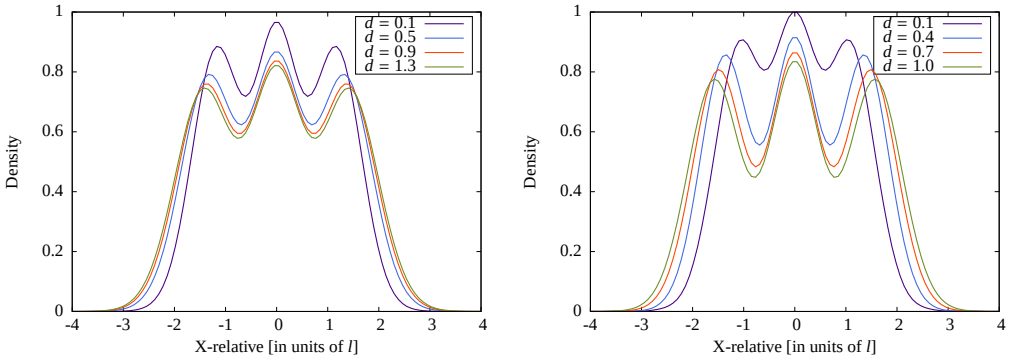

(a) $g = 1$ (b) $g = 3$

Figure 4.2: Density distribution for $N = 6$ fermions in the 1D double trap — comparing the cases with different d for a fixed g.

Firstly, we fix the interaction strength g and examine the density distributions at several distinct d values (Fig. 4.2), which corresponds to the case in the energy profile (Fig. 4.1a). The density seems to be a “mountain” with three “peaks”, and the central “peak” is a bit higher than the other two. The heights of the peaks and their widths are affected by changing parameters d and g. The three peaks

emerge more separated and localized, with roughly equal heights at larger d. This implies that at larger d, the particles have been pushed apart from each other for reducing the repulsive forces. Since the attractive forces only play a minor role when d is larger, the particles' behaviour is dominated by the repulsions. This feature becomes more prominent for the case $g = 3$ (Fig. 4.2b).

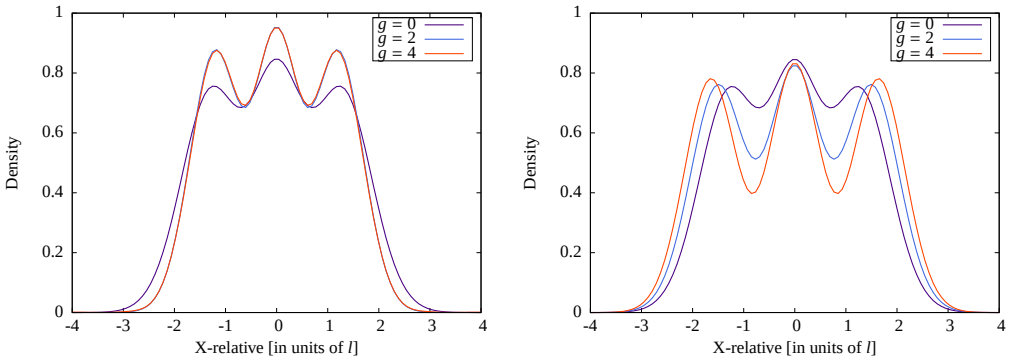

(a) $d = 0.2$ (b) $d = 1$

Figure 4.3: Density distribution for $N = 6$ fermions in the 1D double trap – comparing the cases with different g for a fixed d.

Similarly, we plot the density with fixed d at $d = 0.2$ and $d = 1$ for different g, in analogy with the energy profile (Fig. 4.1b). At $d = 0.2$, despite the peaks growing as g increases, the peaks actually still appear at the same places as without interactions. In other words, the central position of the peaks are not shifted. Moreover, the distribution keeps its general form as we further increase g. This can be seen from the case $g = 4$, which is almost indistinguishable from the one with $g = 2$ (Fig. 4.3a). The situation becomes different when the separation distance is increased (Fig. 4.3b). With a larger separation $d = 1$, the attractive force that can bound the particles at their original places is not strong enough against the repulsive ones. As a result, particles have been pushed further away from each other. Both cases show that the peaks become more localized with interactions, but they choose quite different ways to optimize the energy. The transition of mapping particles from $d = 0.2$ to $d = 1$ is smooth — no threshold value for d can be found to distinguish these two cases.

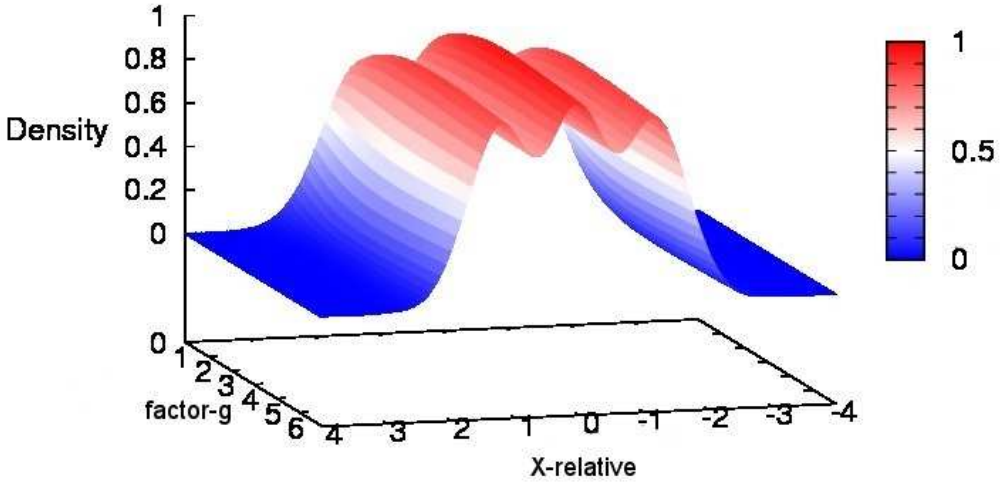

(a) $d = 0.2$

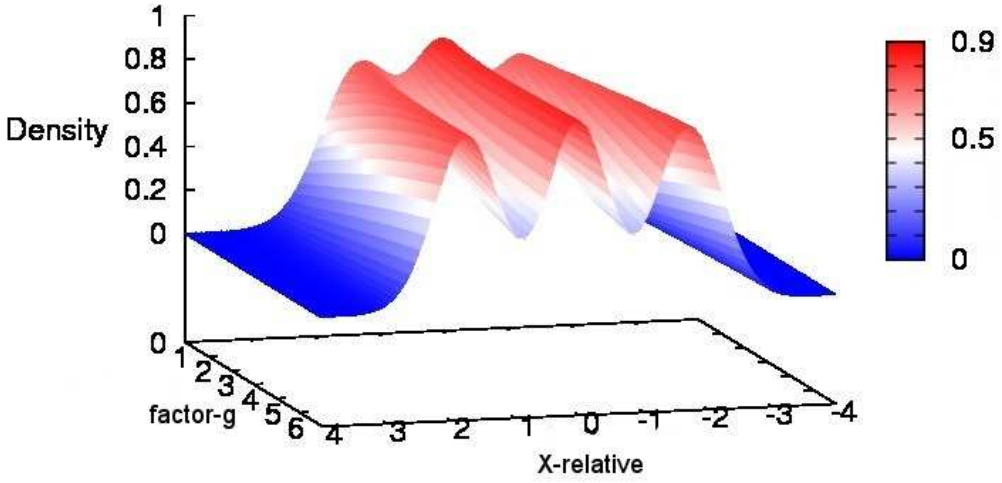

(b) $d = 1$

Figure 4.4: "Landscape" distribution for 6 fermions abtained by continuous change of factor g.

In order to see the change in density as a function of the factor g, we plot the distributions into a "landscape", (Fig. 4.4) which is obtained by piling up the distributions for different g factors. The same conclusion would be drawn as before: by increasing the factor g, the particles can not be pushed apart with a "small" separation (Fig. 4.4a), while they can be separated with a "large" separation (Fig. 4.4b).

4.1.3 The pair-correlation density

Pair-correlation density differs from the normal density distribution, because a pre-condition is introduced (it is commonly called conditional density). In practice, we define one of the particles as the reference, and fix it at a certain position. This condition might cause density deformation for the remaining $N-1$ particles. To find a proper position of the reference particle, the reference point is chosen at a place where the density has a maximum, because in this case we can have a high probability to find a particle at this point. In addition, we usually avoid the central points. The reference at an off-central place can break the symmetry of the distribution, which benefits the comparison between pair-correlation distribution and density distribution.

To explore the conditional density of our system (Fig. 4.5), we choose as one of the possible reference points, the one at around $x = 1.5$ which satisfies all the conditions (found in Fig. 4.3a). The fixed particle could be electron or hole, the property of the reference particle will not affect the results. However, the distribution for the two traps are different, thus in each pair-correlation plot we display the distributions for both traps.

The observation that the particles' mapping is affected by the separation distance is further clarified by comparing the pair-correlations. As an example of a non-interacting case, we show in Fig. 4.5a, its pair-density distribution which without the reference particle is the same as its density distribution. However as g increases, since we have fixed a reference particle at the peak position where the attraction force is stronger than anywhere else, the corresponding peak is found to rise to a higher height than is the case in the density profile. Due to the deformation caused by attractions, this behaviour can be seen more clearly when g becomes larger (Fig. 4.5e).

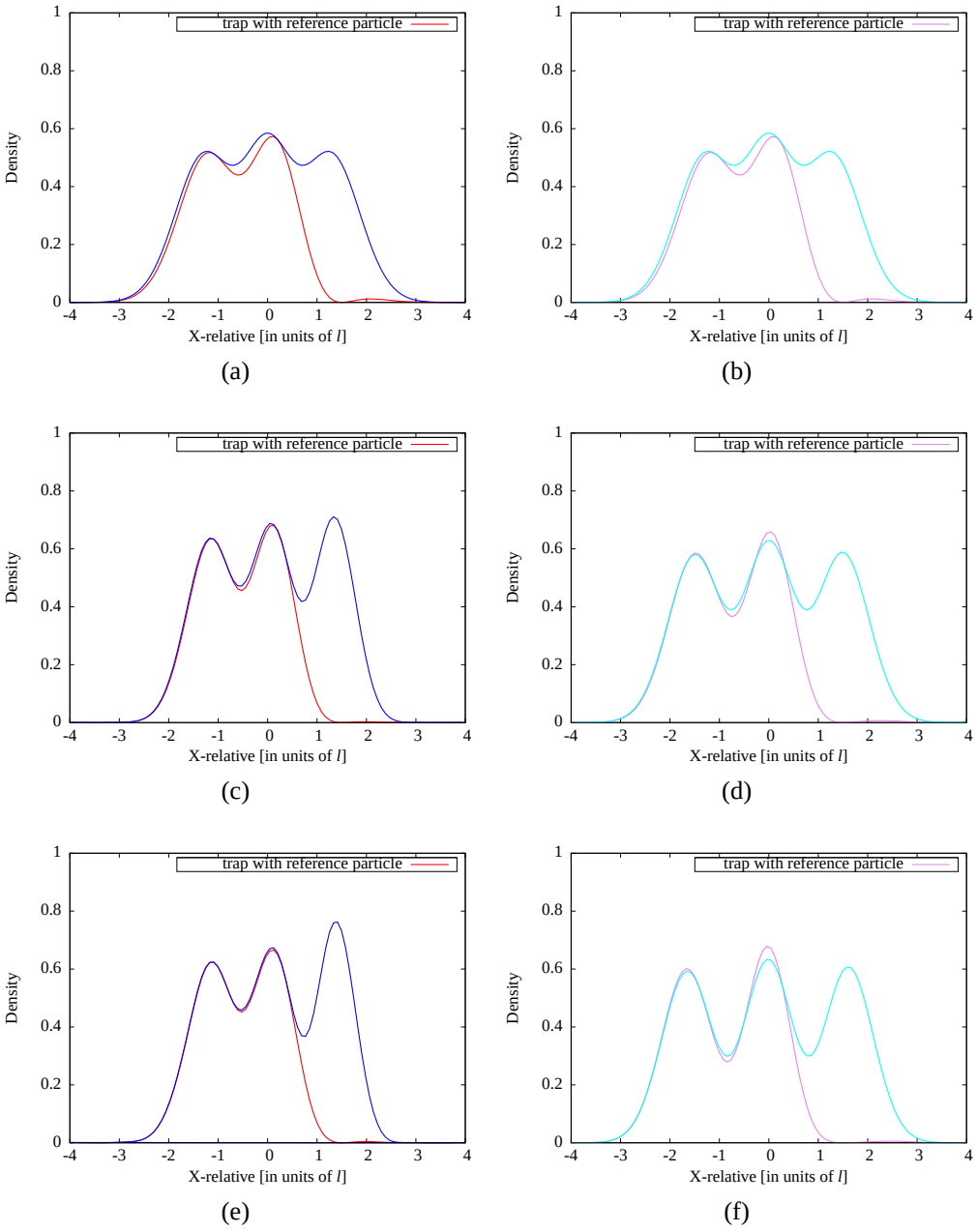

Figure 4.5: Pair-correlation density in the double 1D trap with the reference particle fixed at the point $x = 1.5$. The first column 4.5a, 4.5c, 4.5e is plotted for $d = 0.2$ and the factor g equal to 0, 2, 4 respectively. The second column 4.5b, 4.5d, 4.5f is plotted for $d = 1$ by using the factor g to be equal to 0, 2, 4 respectively.

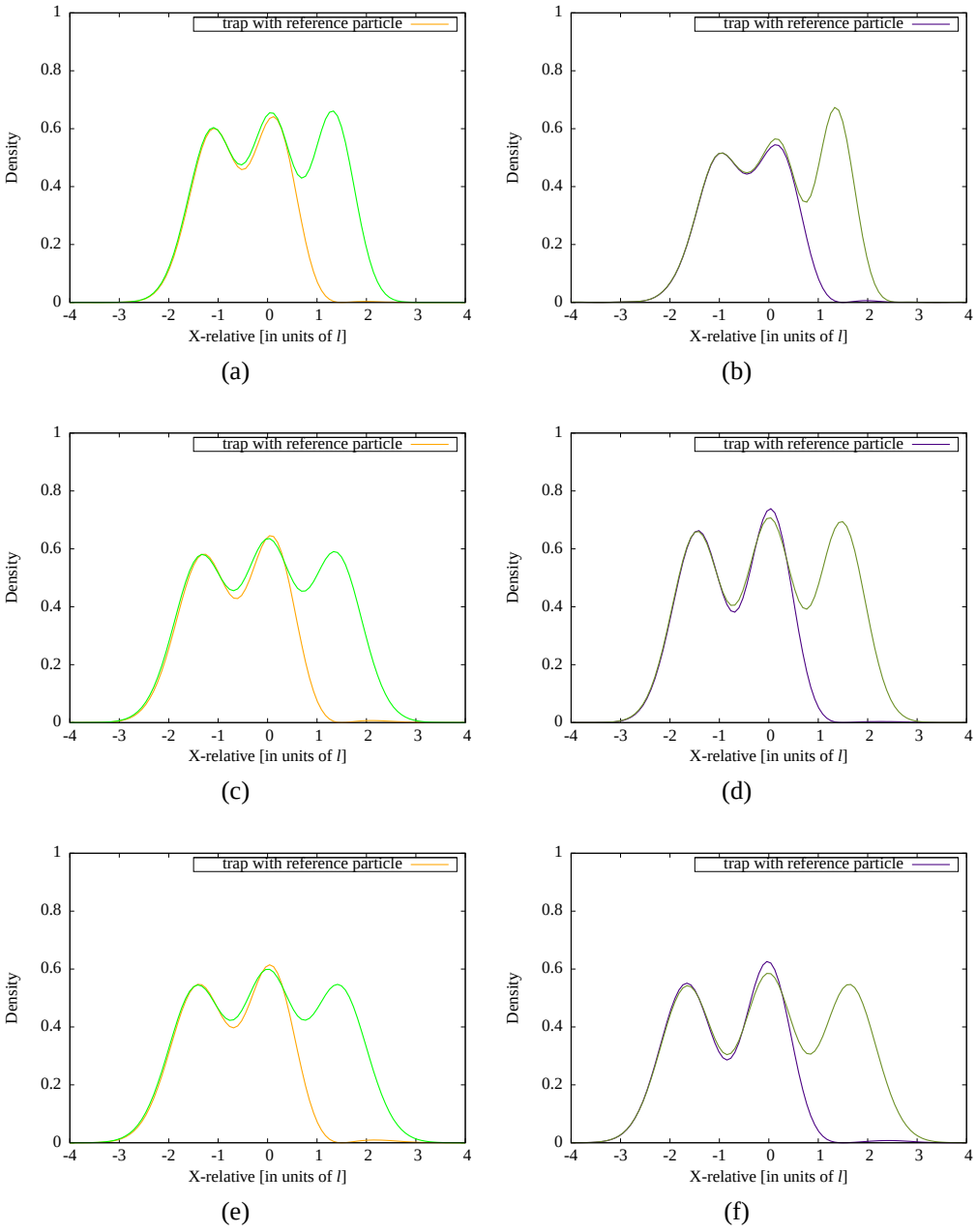

Figure 4.6: Pair-correlation density for $N = 6$ fermions in the double 1D trap with the reference particle still fixed at point $x = 1.5$, The first column Fig. 4.6a, Fig. 4.6c, Fig. 4.6e is plotted for $g = 1$ and the separation d equal to 0.1, 0.6, 1.4 respectively. The second column Fig. 4.6b, Fig. 4.6d, Fig. 4.6f is plotted for $g = 3$ and the separation d equal to 0.1, 0.6, 1.4 respectively.

Fig. 4.5 also demonstrates that the distribution of one trap is strongly affected by the other one, if the separation distance is "small" enough. In this case, the particles of two traps "talk" to each other. For "large" d case as mentioned before, the distribution is the same as before. The reason is because the reference (fixed) particle can not affect the other one's distribution.

To see the affection only by g, we compare the Fig. 4.6c and Fig. 4.6d. They are both plotted for $d = 0.6$, the reference particle can not break the symmetric distribution with $g = 1$, but it causes the far right peak to be higher than the far left peak with $g = 3$. Therefore in the double trap it is the combination of both d and g that cooperate to determine how strong the interactions are (Fig. 4.6).

In summary, we have discussed the numerical results for double 1D system. From the energy profiles, we have found that at any d value, increasing g would reduce the ground state energy. Increasing the separation d would increase the ground state energy, but it will be saturated if g increases even more. The density profiles show clearly how the separation parameter d influences the ground state distributions.

4.2 Single 1D trap with bosons or fermions

From the previous section, we know that if the separation between the two traps is large enough, we could neglect their mutual attractive interaction, thus the double trap becomes analogous to two isolated single traps. In the single 1D trap, we can leave out the parameter d and just focus our attention on the factor g and thus isolate the role of this parameter. Apart from that, this simple model will give information about similarities and differences arising from statistical rules (fermions or bosons). In doing so, Coulomb interaction as well as contact interaction[1] are used in this study.

The interaction strength g plays a key role in the single 1D model. We sweep the factor g in quite a large range, and compare the ground state energy thus obtained for both fermions and bosons. We find (Fig. 4.7) an energy difference only in the weekly interacting region. The bosons' energy exactly equals that of the fermions' from $g > 2$.

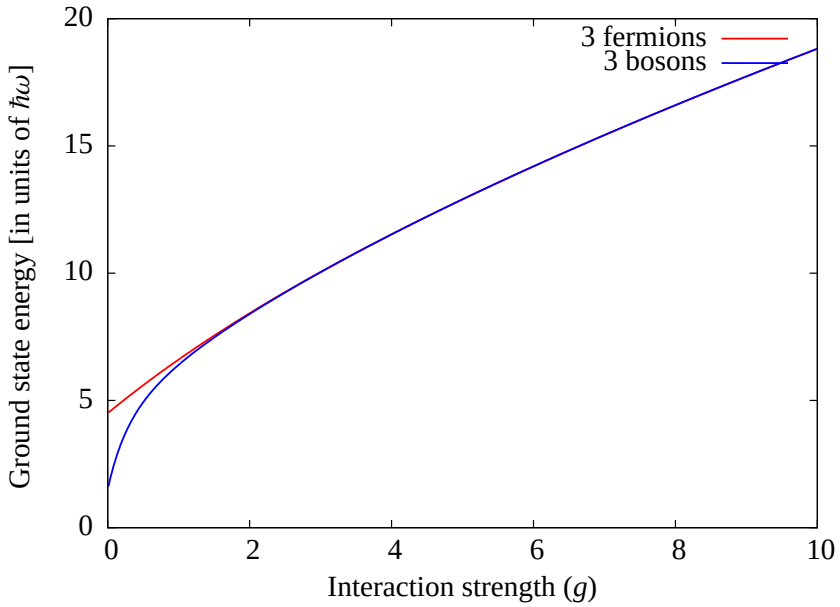

Figure 4.7: A comparison made of ground state energy of bosons and fermions by changing factor g from 0.01 to 10.

[1]The contact interaction is a kind of very short range interaction.

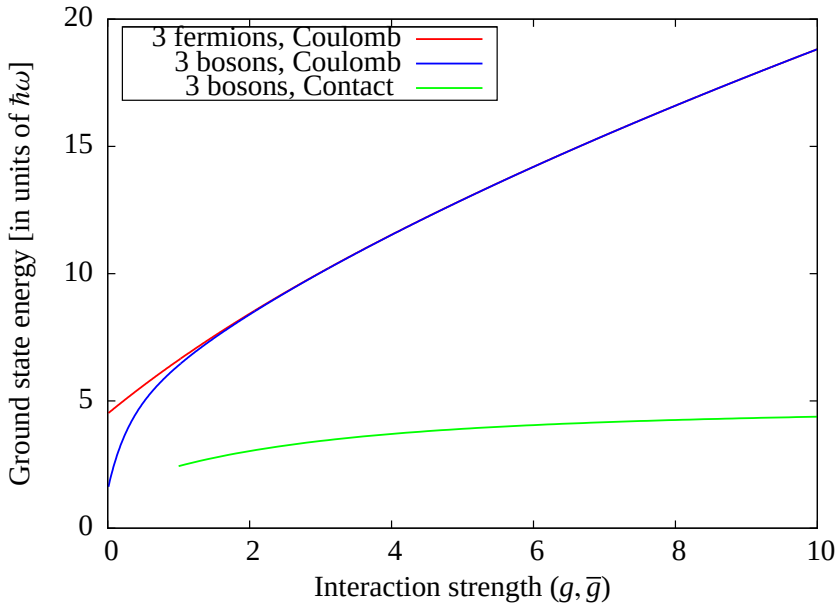

Figure 4.8: The density distribution with contact interaction for bosons, compared with the Coulomb interaction both for fermions and bosons.

Another kind of interaction called contact interaction (or known as δ potential) has been broadly used for bosons. For the dilute gas (also can be used for this finite system), at low energy the interaction is primarily two-body and we can write $V(r' - r)$ as

$$V(r' - r) = \bar{g}\delta(r' - r) \tag{4.1}$$

where the interaction strength is characterized only by a single parameter, the s-wave scattering length α. To distinguish this kind of interaction from Coulomb interaction, we use $\bar{g}$ for the contact interaction strength

$$\bar{g} = \frac{4\pi\hbar^2\alpha}{M}. \tag{4.2}$$

In order to compare the Coulomb interaction with contact interaction, we consider their energy profiles obtained by sweeping g and $\bar{g}$ in the same range (Fig. 4.8). In the contact interaction case, the ground state energy tends to be reached quickly. As the repulsion forces the particles to move apart from each other, they have much less chance to occupy the same position. Since $V(r' - r)$ contains a delta function, the particles would not have any interaction if they are at different r. Thus the ground state energy would not be very sensitive to the interaction strength when $\bar{g}$ increases further.

The density distribution in Fig. 4.9 is plotted for the case of 3 bosons in 1D single trap with contact interaction. We do not show the non-interacting case ($\overline{g} = 0$). The non-interacting distribution for bosons will give an infinitely high and infinitely thin spike at the origin. In order to be comparable, the distribution has to have a finite size in both scales. Therefore, we let $\overline{g}$ vary from a relatively small value but not from zero. The case for $\overline{g} = 1$ is a normalized Gaussian distribution. Although the ground state energy changes only slightly when $\overline{g}$ increases, the density distribution deforms dramatically from a single peak into three peaks.

Fig. 4.10 shows what happens by using the Coulomb interaction instead of the contact interaction. Compared to the contact case, the deforming range of g in the Coulomb case is roughly from 0 to 1. Thus we find out the interesting range for factor g to examine the fermionization behaviour (see below).

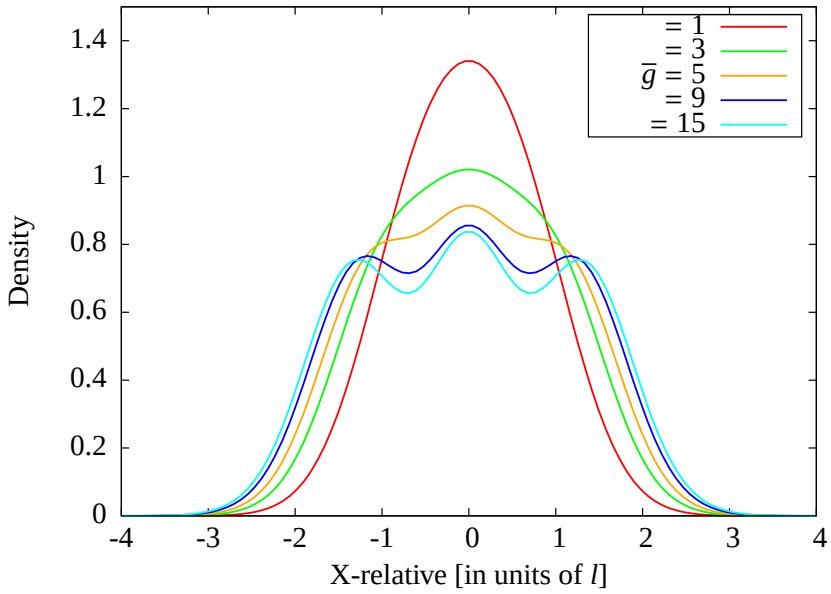

Figure 4.9: Density distribution for $N = 3$ bosons in a single 1D trap by using the contact interaction. Distinct differences can be seen for different $\overline{g}$.

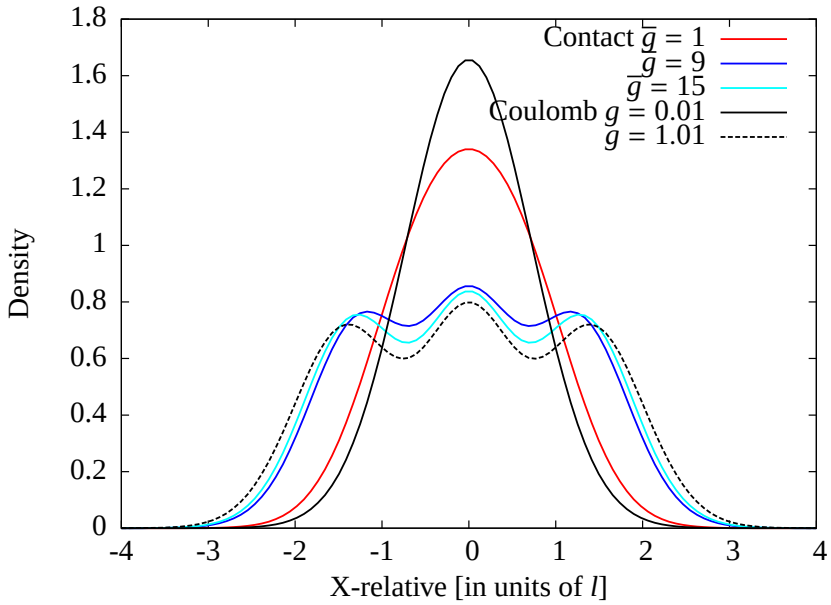

Figure 4.10: Density distribution for $N = 3$ bosons in 1D single trap and comparison of the deformation region for contact interaction and Coulomb interaction.

4.2.1 Fermionization: comparison of the density distribution of bosons and fermions in a single 1D trap

As we have already seen in some plots, if the interaction strength becomes larger, the distributions for bosons look more and more like those for fermions [16], both in contact and Coulomb cases. We would now like to examine in more detail how close the density distributions for bosons and fermions can be under the same conditions.

Fig. 4.11 shows that as g increases, the boson distribution is already very close to fermion case up to $g = 1.01$, and that the two distributions are almost identical at the large g limit.

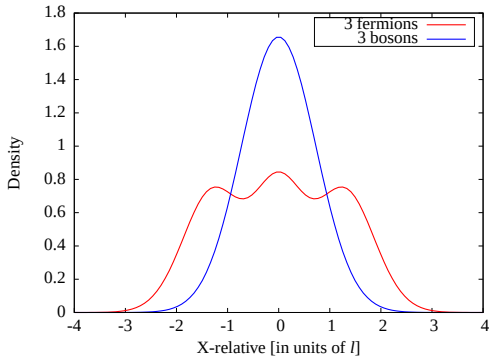

(a) $g = 0.01$

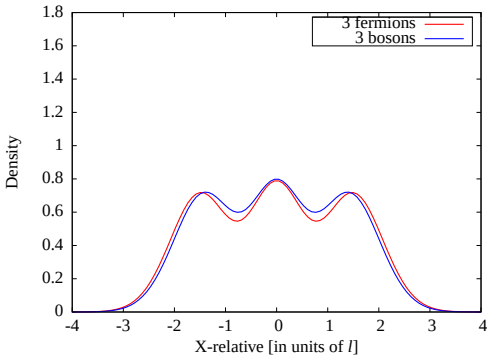

(b) $g = 1.01$

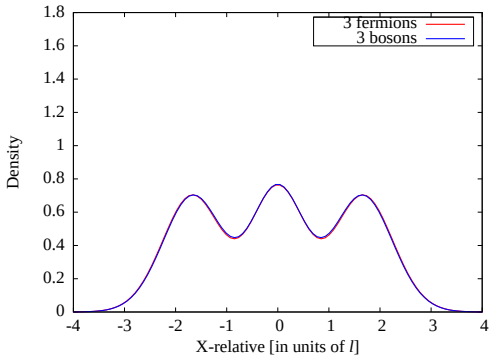

(c) $g = 2.01$

Figure 4.11: Density distribution for bosons and fermions in a single 1D trap for various values of factor g.

The fermionization behaviour is easy to understand: in order to minimize their mutual repulsion, bosons are forced apart from each other so as to prevent the occupation at the same position. This scenario is very similar to the Pauli exclusion for fermions. In this context, the bosons resemble some fermionic properties. One system for such a boson gas has been proposed since 50 years ago, namely Tonks-Girardeau gas [22, 23].

In summary, firstly we have investigated some basic properties in a single 1D trap. We have found that it is different from double 1D trap. The ground state energy for the single 1D trap is always increasing as g increases. The density distribution for a single trap is very similar to the case with large d in the double trap. Moreover, we do find fermionization behaviour in the single 1D trap, where the boson and fermion density profiles are strikingly similar, in the limit of large interaction strength. Therefore, we now return to the double trap model and in the

next section examine this fermionization behaviour in some detail.

4.3 Double 1D trap with bosons

In this section, we wish to answer the following questions:

- Does the double 1D trap exhibit fermionization similar to that of the single 1D trap?
- If so is the case what are the major parameters involved?
- How does the separation d affect fermionization?

4.3.1 The energy of the ground state for bosons

We consider the energy profiles. In order to see in what region of each parameter the bosons and fermions show similar behaviour, in the same spirit as for the fermions, we separately vary the separation distance and interaction strength in the bosonic case. According to Fig. 4.12a, the energy for bosons and fermions largely agree in any range of d. For $g = 1$, they "run" in parallel, the fermions having slightly higher energy. For $g = 3$, both are exactly running in the same "track". On the other hand, with increasing g (Fig. 4.12b), the same energy is obtained for bosons and fermions only with larger g. In the weak interacting range, the boson energy is lower than the fermion energy, which is in accord with what we get in $g = 1$ case. What is interesting for bosonic energy is that it increases for small g, and then decreases for larger g and overlaps with fermionic energy.

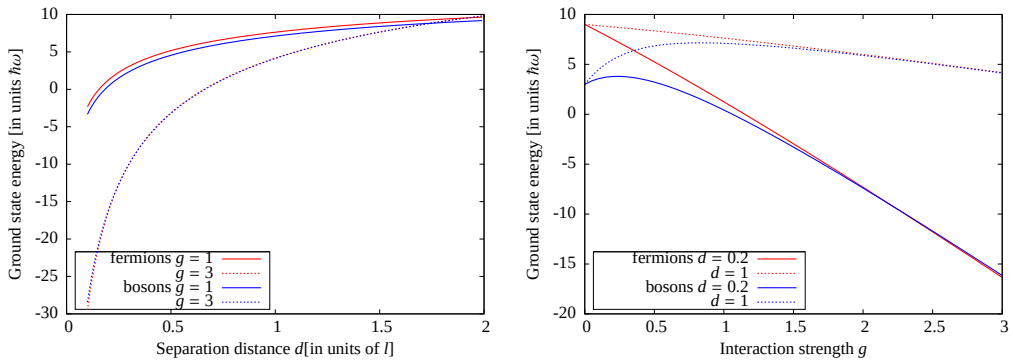

(a) fixed g,varying d (b) fixed d,varying g

Figure 4.12: The comparison of ground state energy for $N = 6$ fermions and $N = 6$ bosons in the double 1D trap.

4.3.2 The density distribution for bosons

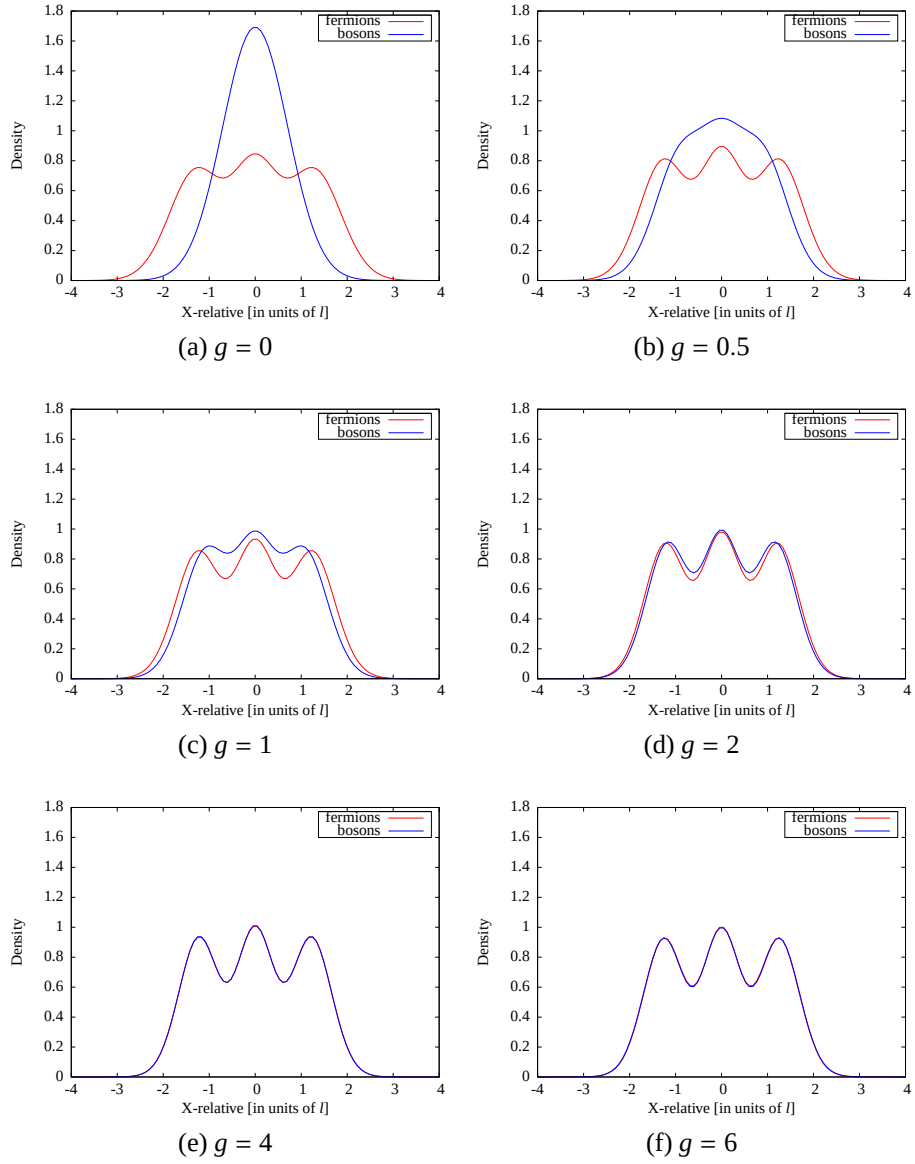

(a) $g = 0$ (b) $g = 0.5$

(c) $g = 1$ (d) $g = 2$

(e) $g = 4$ (f) $g = 6$

Figure 4.13: Comparison of the density distribution for bosons and fermions in a double 1D trap with $d = 0.2$.

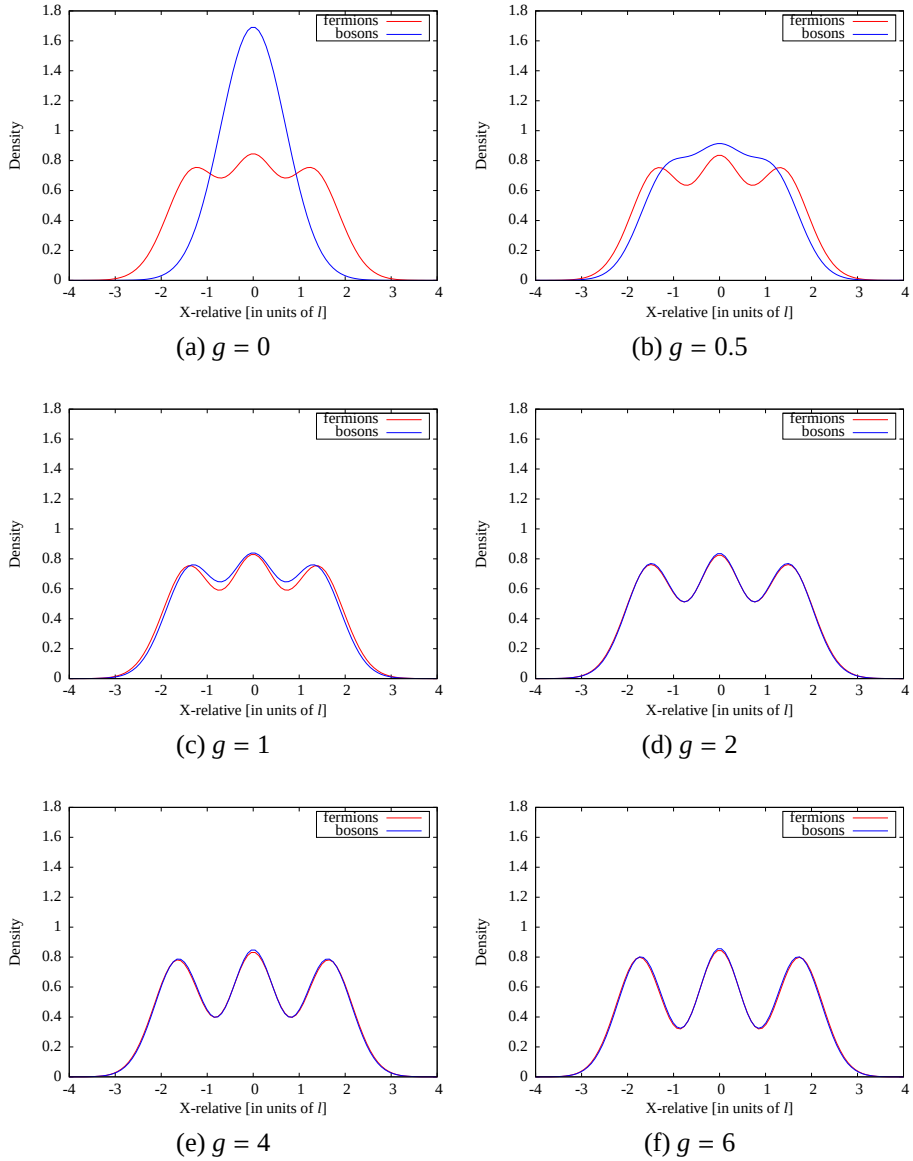

(a) $g = 0$ (b) $g = 0.5$

(c) $g = 1$ (d) $g = 2$

(e) $g = 4$ (f) $g = 6$

Figure 4.14: Comparison of the density distribution of bosons and fermions in a double 1D trap with $d = 1$.

According to Fig. 4.13 and Fig. 4.14, the fermionization takes places both in the cases of $d = 0.2$ and $d = 1$. When factor g is increased, the Gaussian-like distribution of bosons deforms quickly, and later joins the fermionic distribution. The value of interaction strength needed to achieve fermionization is different for $d = 0.2$ and $d = 1$. For small d case, we see that a higher g is required to get the

same distribution than for the case of large d.

We can conclude this section with the answers:
The bosons can be fermionized in the double 1D trap. The same conclusion is reached for single 1D trap, where this behaviour is controlled by the increasing of interaction strength. The separation d can also affect fermionization in the sense that this behaviour is slowed down for small d. Moreover, we find that the ground state energy for bosons would be first increasing as we add the interactions, which is in sharp contrast with the linearly decreasing behaviour of fermionic energy.

4.4 1D trap with ideal dipoles

Dipolar system[2] is another widely investigated model which has many interesting features, especially in low dimensions [11]. Many parameters of such a system can be controlled experimentally. In Fig. 4.15, the dipole tilt angle can be aligned by an external field in a two dimensional harmonic trap. The ideal dipole-dipole interaction can in this manner be tuned and swept from attractive to repulsive via this external field.

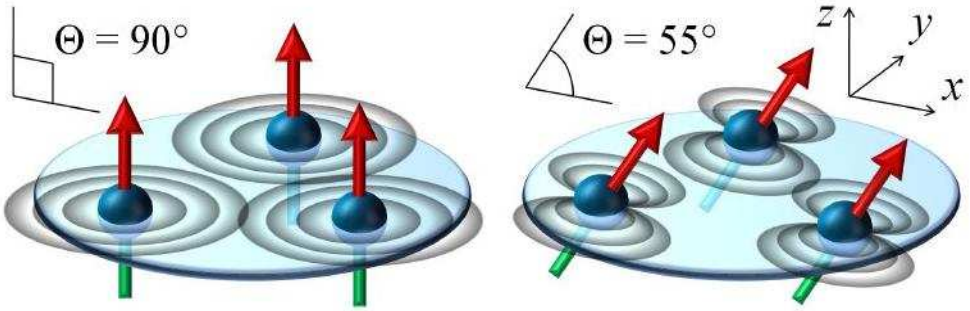

Figure 4.15: (taken from Ref. [9])
A schematic diagram of a few dipoles in a harmonic trap, the dipole angle can be tuned by an external field.

A particularly interesting case is a 1D trap with dipoles' angle Θ aligned to 90°. Consider a 1D double trap with attractive Coulomb force, where the electrons and holes are also aligned perpendicularly. Therefore, an electron and hole couple can be analogous to an ideal dipole. Though the definition of dipole-dipole interaction has many differences from the Coulomb interaction, maybe we can try to make a qualitative comparison between these two models. A short description of dipole interaction can be found in Appendix B. Here we only point out that the increasing repulsive region corresponds to the dipole angle Θ from 0.304π to 0.5π.

We might encounter a problem, if as we tune the angle in order to change the interaction strength, Θ would no longer remains at 90°, which is not the analogous case for the electron-hole model as we assumed. However, the dipole in this model

[2] All the results for dipolar system have been obtained by my colleague J. Bjerlin. More systematic calculation for this system can be found in his master thesis "Dipole-Dipole Interaction in Quasi One-Dimensional Harmonic Traps".

has been simplified and taken as an ideal particle. Therefore tuning the dipole angle only means changing its interaction strength.

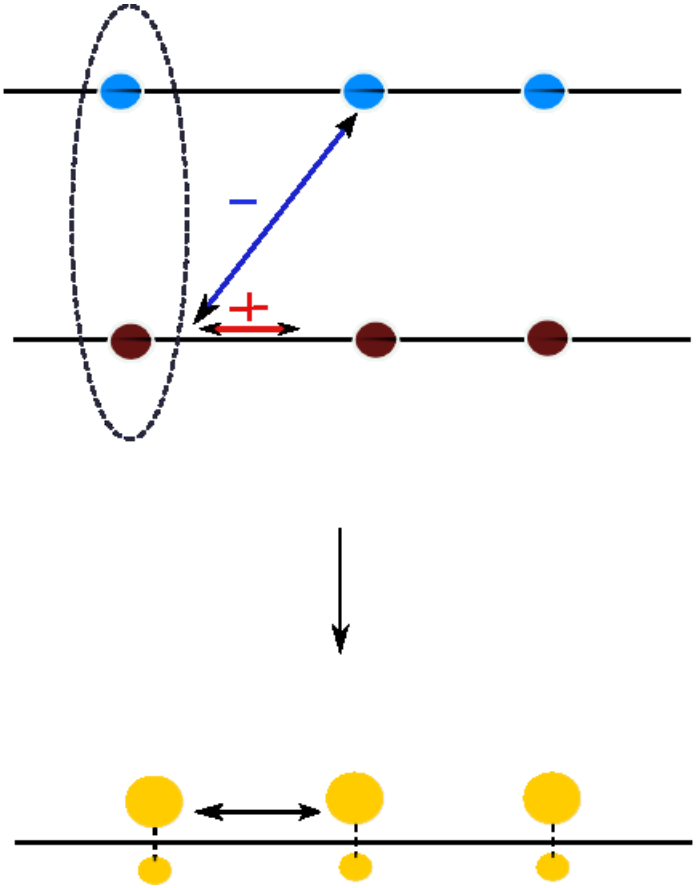

Figure 4.16: The similarity between Coulomb system and dipole system.

4.4.1 The energy spectrum comparison between different 1D models

In the energy profile, the absolute value has no meaning. Instead we must pay attention to the relative changes and energy splittings as the interaction strength is varied. For the dipole case, Fig. 4.17 shows the energy spectrum for $N = 3$ ideal fermion dipoles in a quasi 1D trap. The degeneracy appears for the non-interacting case. By increasing the dipole interaction strength $\bar{d}$, the energy gets increased.

Recalling that the energy of the double 1D trap model decreases with increasing the factor g indicates that the double 1D trap and dipolar 1D with repulsive interaction behave quite differently. The reason we didn't explore the excited state property of the double 1D model is again because of the convergence problems and the large amount of required computing time.

We have only displayed the simulated results of energy spectra for single 1D trap model, since it is less time-consuming than the double 1D trap. According to Fig. 4.18, the fermionization behaviour shows up again: the bosons can have the same energy as the fermions not only for the ground state but also for the first several excited states. Since in contrast with the case of bosons, the energy of fermions increases linearly, we find that the single 1D trap with bosons can be analogous to the case of dipoles. The actual values differ, but the qualitative similarity of the excited states is clear, and their energies split at the origin for both cases.

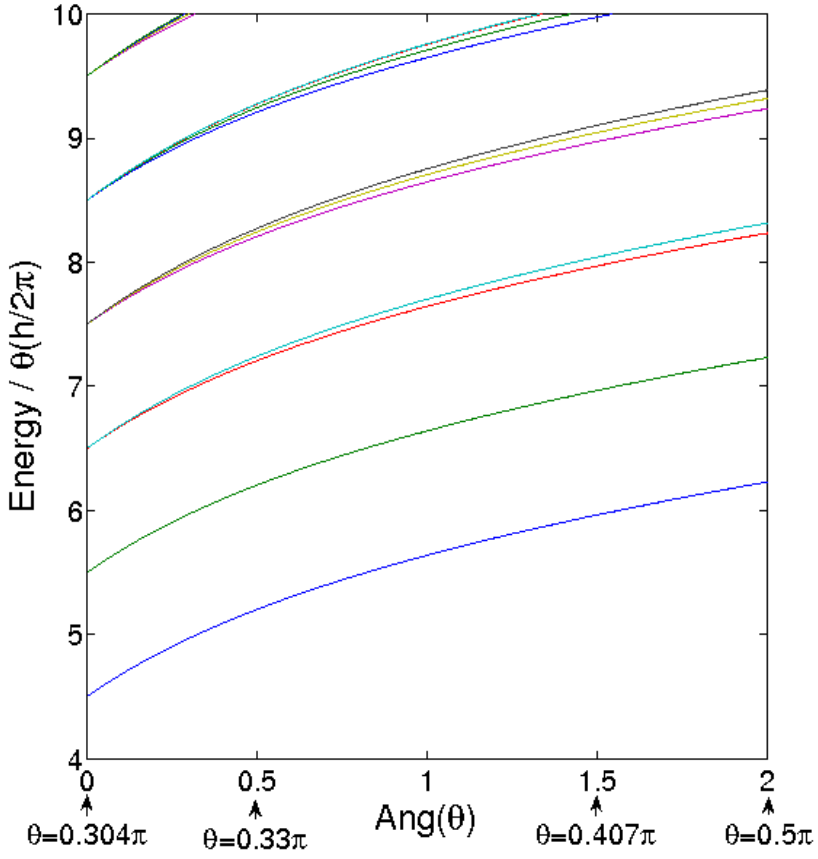

Figure 4.17: (taken from Ref. [11])
Energy spectrum for $N = 3$ ideal fermion dipoles in a quasi 1D trap.

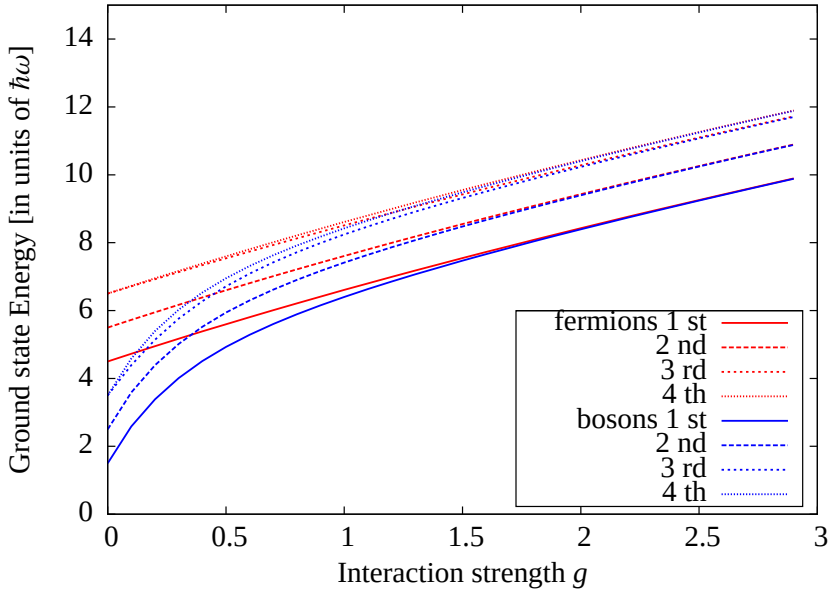

Figure 4.18: Energy spectrum for $N = 3$ particles in the single 1D trap by tuning g from 0 to 3.

4.4.2 Density distribution for ideal dipoles

The dipole-dipole interaction has many similarities with Coulomb interaction. Here we focus on the fermionization behaviour. According to Fig. 4.19, the distribution for bosons has a Gaussian-shaped profile for non-interacting case. As the interaction strength increases up to 3, one could find 4 fully localized peaks, each independent of the others. The fermionization of mapping is seen as a general phenomenon for these comparable models. We have already shown that such feature could happen in the system of double 1D trap and single 1D trap by Coulomb interaction. However, there are still some differences. For the double 1D trap, increasing the interaction strength can not let the bosons peaks remain completely separated. They undergo localization in some sense for sure, however, with attractive force the behaviour for double 1D model is basically different: the peaks are confined in a Gaussian-shaped profile, where in other two cases (single 1D trap with Coulomb interaction and 1D with dipole interaction) the peaks are becoming fully independent.

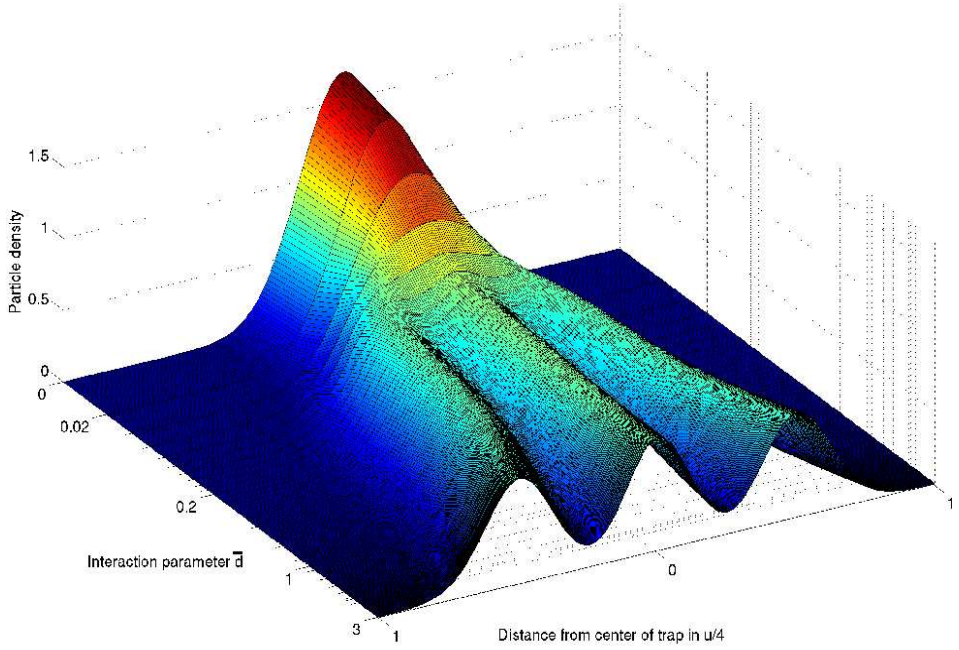

Figure 4.19: (taken from Ref. [11])
A wedding-dress-shaped density for the case $N = 3$ ideal boson dipoles in a quasi 1D trap.

To summarize, we have made a comparison of energy spectrum for two models: the single 1D trap with dipole-dipole interaction and the single 1D trap with Coulombic interaction. Since dipolar and Coulombic interactions are primarily repulsive (if particles all with the same sign of charges), the energy is growing as g increases in both cases. Moreover, we found that the fermionization behaviour of mapping from bosons-like to fermions-like is not only for the Coulomb interaction, it is also seen in the diple-dipole interaction model.

Chapter 5

Conclusions and outlook

In this project, I mostly focus on the behaviour of electron-hole systems in double 1D harmonic traps with Coulomb interaction. The sensitivity to and the influences of the changes of two parameters (separation distance d and Coulomb interaction strength g) have been discussed via energy profile and density distribution profile. When the wavefunctions have no overlap between the two traps, each trap can be considered as an 1D system. We compare some of the results obtained from this model with other 1D systems, including single 1D and 1D dipolar systems. In particular the fermionization behaviour is a common feature seen via the comparison of density distribution profiles.

One of the prominent features in the double trap model is that the total energy becomes favourable as g increases. Besides, two values of separation distances ($d = 0.2$ and $d = 1$) cause different response as g increases. We find that for the large separation d, the same mapping behaviour is obtained as for the single 1D trap, which makes perfectly sense because the single 1D trap is a simplified version of the double 1D trap, as the (attractive) interaction between the two traps is ignored.

We also find that under a certain condition (if the interaction strength is large enough) some of the results seem to be blinded to the statistical rules, in the energy plot as well as the density plot — the bosonic and fermionic cases look similar.

Despite many successes of the CI method, there are still some natural shortcomings. Especially in the double trap model the convergence becomes a considerable issue and makes it almost impossible to treat the case of more than 6 particles. Moreover we have a limited range for each parameter which does not allow us to investigate the case with extremely small separation or strong inter-

action strength. For the same reason, the "geometry factor" can not be properly studied. In principle as we loosen or tighten the condition of radial freedom (but still in the quasi-1D region), the result will be different for sure. However as the theoretical uncertainty is taken into account, it becomes difficult to draw any definite conclusions on this matter.

It remains much work to be done to investigate the properties of electron-hole systems. If more care be paid on Fig. 5.1, we might find out the distance between the electrons and holes is controlled by the electronic field which has the direction to be perpendicular to the quantum well plane. The stronger voltage bias the far separated the electrons and holes can be. Therefore, d should be replaced by a function of the electric field, however, the d parameter in our simple model has been changed artificially. Moreover, the electron-hole pairs are perpendicular to the axial direction due to the static-electric force. To design un-perpendicular electron-hole pairs for a few-body system, the simple way is to pose unequal numbers of electrons and holes in different traps. The primary calculations for such a system can be found (in Appendix C).

To analyze a few-body system, it is beneficial to compare the unit length l with some atomic scales. In our case the unit length was defined from the artificial harmonic oscillator frequencies, but we can also find a way to compare l with the Bohr radius of the pair. In a many-body system it is convenient to define a dimensionless ratio $\bar{\lambda}$ between the radius r_0[1] volume per particle and the Bohr radius. The few body system will then be seen as a "zoom in" to connect with the many body system with the same $\bar{\lambda}$.

[1] r_0 is defined in terms of the volume per particle: $V/N = \frac{4}{3}\pi r_0^3$.

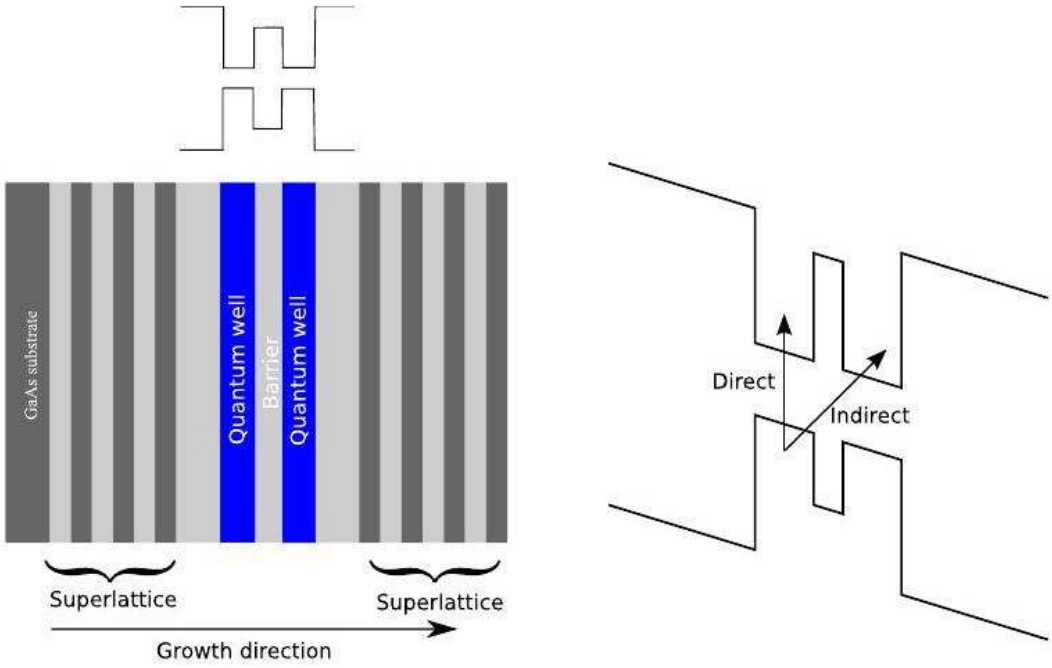

Figure 5.1: (taken from Ref. [17])
A schema of exciton shown in the coupled quantum well, where electrons and holes are separated in two different layers.

An evaluation of my Master Degree Project

I highly appreciate the chance to do my master degree project at the mathematical physics department. To conclude this report, I'd like to reflect on what I have learnt and achieved.

First of all, I find the most interesting area in physics for myself is on the numerical simulation method for Many-Particle systems under the first principle. Unlike any other course projects, students could have maximum freedom of choosing the subject they want to study, not what they have to study. They can be their own master.

Secondly, I have learnt to work in a group. There were countless times I was saved by someone of my group when problems appeared which I couldn't solve by myself. On the other hand, I would be glad to offer help or to give suggestions to someone else. This collaboration was not limited to my supervisor's group, but I could also benefit from knowledge of all the members in the Matfys department and even the entire Physics department; an inspiring network of knowledge.

Moreover, I gained knowledge of some useful software, such as Gnuplot, Inkscape etc. Most people use Matlab for processing data and generating figures, whereas I find there could be a trouble of modifying their captions on the Matlab figures. However, Gnuplot provides a possibility to save the caption and figure into an "eps" file and a "latex" file separately, so it becomes so easy to edit anything on a caption without re-plotting the figure. Besides, once I enclose the selected orders in a file, which could work for all the figures in the same genre, thus highly reducing the repeated work load for me.

Finally, most difficult with my master project was writing a scientific thesis and preparing the defence. As a Chinese student, since we never have the experience of the training how to write a thesis or report in English, I have to start from the lowest rank. Most part of my thesis has been modified several times; each time I correct some mistakes by realizing the corresponding grammar rules. As for the defence, there is no short cut but practising only. The more I organize my talk, the more clearly I could express it. The key point is that, at the end, I really have the confidence and the passion for sharing all of what I have discovered in my project.

Appendix A

CI method in detail

As some of the theory presented in this thesis has been quite brief, this part is a complement to Chapter 3, providing more details for the CI method [14].

The many-particle wavefunction can be constructed from a set of single-particle wavefunctions ϕ_ν.

$$\Psi(r_1, \ldots, r_N) = \sum_{P \in S_N} sgn(P) P\Big(\phi_{\nu_1}(r_1)\phi_{\nu_2}(r_2)\cdots\phi_{\nu_N}(r_N)\Big) \tag{A.1}$$

We represent the many-particle states in terms of these occupied single-particle orbitals ϕ_ν

$$|\Phi\rangle = |n_1, n_2, n_3, \ldots\rangle$$

The completeness theorem says that if the set of single-particle orbitals ϕ_ν is complete, then the sets of symmetric (antisymmetric) wavefunctions Φ created from them are complete as well.

The single and two-particle operators are treated by using the creation and annihilation operators as well as corresponding orbitals; we have:

$$\hat{U} = \sum_{i=1}^{N} \hat{u}_i = \sum_{i,j=1}^{N} \langle i|\hat{u}|j\rangle \hat{a}_i^\dagger \hat{a}_j \tag{A.2}$$

$$\hat{V} = \frac{1}{2} \sum_{\substack{i,j=1 \\ i \neq j}}^{N} \hat{v}_{i,j} = \frac{1}{2} \sum_{i,j,k,l=1}^{N} \langle ij|\hat{v}|kl\rangle \hat{a}_i^\dagger \hat{a}_j^\dagger \hat{a}_k \hat{a}_l \tag{A.3}$$

In order to solve the time-independent Schrödinger equation

$$\sum_k \hat{H}|\Psi\rangle = E|\Psi\rangle \tag{A.4}$$

we may plug in the identity operator $\hat{I} = \sum_k |\Phi_k\rangle\langle\Phi_k|$ and multiply by $\langle\Phi_l|$ from the left side

$$\sum_k \langle\Phi_l|\hat{H}|\Phi_k\rangle\langle\Phi_k|\Psi\rangle = \langle\Phi_l|E|\Psi\rangle \tag{A.5}$$

By using matrix formulation, we obtain

$$\begin{bmatrix} \langle\Phi_1|\hat{H}|\Phi_1\rangle & \cdots & \langle\Phi_1|\hat{H}|\Phi_D\rangle \\ \langle\Phi_2|\hat{H}|\Phi_1\rangle & \cdots & \langle\Phi_2|\hat{H}|\Phi_D\rangle \\ \vdots & \ddots & \vdots \\ \langle\Phi_D|\hat{H}|\Phi_1\rangle & \cdots & \langle\Phi_D|\hat{H}|\Phi_D\rangle \end{bmatrix} \begin{bmatrix} \langle\Phi_1|\Psi\rangle \\ \langle\Phi_2|\Psi\rangle \\ \vdots \\ \langle\Phi_D|\Psi\rangle \end{bmatrix} = E \begin{bmatrix} \langle\Phi_1|\Psi\rangle \\ \langle\Phi_2|\Psi\rangle \\ \vdots \\ \langle\Phi_D|\Psi\rangle \end{bmatrix} \tag{A.6}$$

Diagonalising this matrix gives the energy eigenvalues E and the expansion coefficients $\langle\Phi_i|\Psi\rangle$. By knowing the expansion coefficients, we can now construct the full many-body wavefunction by using

$$\langle r|\Psi\rangle = \sum_k \langle r|\Phi_k\rangle\langle\Phi_k|\Psi\rangle \tag{A.7}$$

Thus using post-processing CI method, the many-body wavefunction gives us information about several quantities, such as particle density and pair-correlated density, both in the coordinate space. The particle density at a point r is given by

$$P_\Psi(r) = \langle\Psi| \sum_{i,j} \phi_i^*(r)\phi_j(r)\hat{c}_i^\dagger \hat{c}_j|\Psi\rangle \tag{A.8}$$

The pair-correlated density can be calculated if we in addition introduce a particle at position r'

$$P_\Psi^c(r, r') = \langle\Psi| \sum_{i,j,k,l} \phi_i^*(r)\phi_j(r)\phi_k^*(r')\phi_l(r')\hat{c}_i^\dagger \hat{c}_j \hat{c}_k^\dagger \hat{c}_l|\Psi\rangle \tag{A.9}$$

Appendix B

System description for ideal dipoles in a quasi 1D trap

In this section, we will briefly introduce the Hamiltonian of 1D system for ideal dipoles with dipolar interaction.

The many-particle Hamiltonian for such a system is

$$\hat{H}^{tot} = \hat{H}_{kin} + \hat{H}_{ext} + \hat{V} \tag{B.1}$$

where as before the quantities in the right-hand side denote the kinetic , external potential and interaction term respectively.

The $\hat{H}_{kin}$ and $\hat{H}_{ext}$ are given by

$$\hat{H}_{kin} + \hat{H}_{ext} = \sum_{i=1}^{n} \Big(\frac{\hat{p}_i^2}{2m} + \frac{1}{2} m \Big(\omega^2 x_i^2 + \omega_\perp^2 (y_i^2 + z_i^2) \Big) \tag{B.2}$$

After going through some tedious calculations [11] the interaction term can be obtained as

$$V_{1D}(x) = D(\theta, \bar{d}) \Big(\sqrt{2\pi}(x^2 + 1) e^{\frac{1}{2}x^2} erfc(\frac{x}{\sqrt{2}}) - 2z \Big) + \frac{2d^2}{3l_{\perp p}^2} \delta(x) \tag{B.3}$$

The interaction coefficient $D(\theta, \bar{d})$ depends on two variables θ and $\bar{d}$. In a classical picture, the ideal dipole is defined as the limit of two opposite point charges moving infinitely close to each other. Since dipole moment is $\bar{p} = q \cdot \bar{d}$, $D(\theta, \bar{d})$ can be written in the form of

$$D(\theta, \bar{d}) = -\frac{\bar{p}^2}{4\pi\varepsilon_0} \frac{1}{8 l_p^3} (1 + 3\cos 2\theta) \tag{B.4}$$

where $\overline{d}$ is given in the units of Debye, l_p is the oscillator length of the external confinement. It indicates that the changes of θ (the angle between dipole moment vector $\overline{p}$ and 1D axial x) can not only affect the magnitude of $D(\theta, \overline{d})$ but can even flip the sign. At a particular value (so called the critical angle) this expression vanishes (equvalently $1 + 3\cos 2\theta = 0$) , we obtain $\theta_{crit} \approx 0.304\pi$ or 54.7°.

For $\theta < \theta_{crit}$, the interaction force between the two dipoles is attractive, by contrast for $\theta > \theta_{crit}$, the interaction force changes to be repulsive. Since the analogous case for our double trap system is the dipole moment perpendicular to the axial direction, which gives $\theta = \pi/2$, it is evident that the dipole-dipole interaction in this case is repulsive.

Appendix C

Additional figures for double one-dimensional harmonic trap

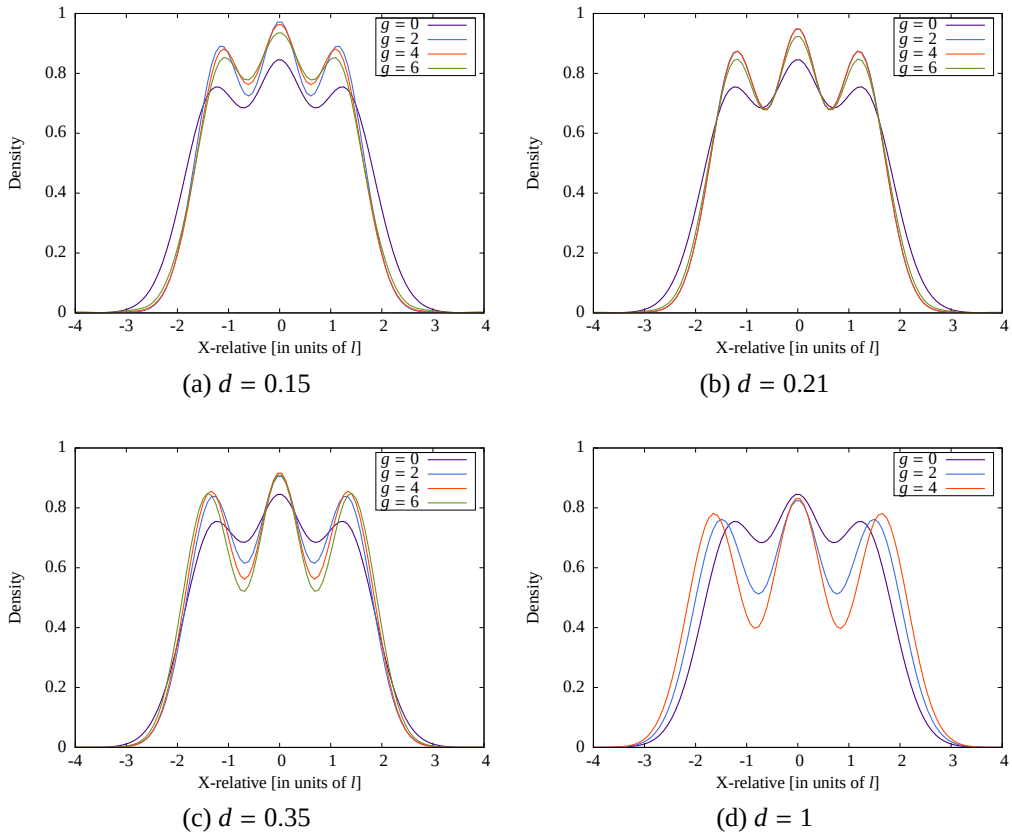

(a) $d = 0.15$ (b) $d = 0.21$

(c) $d = 0.35$ (d) $d = 1$

Figure C.1: Double 1D trap for fermions with different values of d and g.

Fig. C.1 indicates the reason for our choices of d ($d = 0.2$ and $d = 1$) as increasing g. When d is around or smaller than 0.2 (Fig. C.1a and Fig. C.1b) the peaks get closer together like an integrated distribution. When d goes far beyond 0.2 (Fig. C.1c), the distribution has deeper valleys and the peaks are more localized. Note that there is no sharp transition for any d values, Therefore, we show the distributions for $d = 0.2$ and $d = 1$ to emphasize the underlying diferences.

Fig. C.2b intends to show the continuous deformation for bosons distribution as d changes. However, it is hard to visulize the "valley" in Fig C.2b and compare it with Fig C.2a. For this reason, they are not included in the previous section.

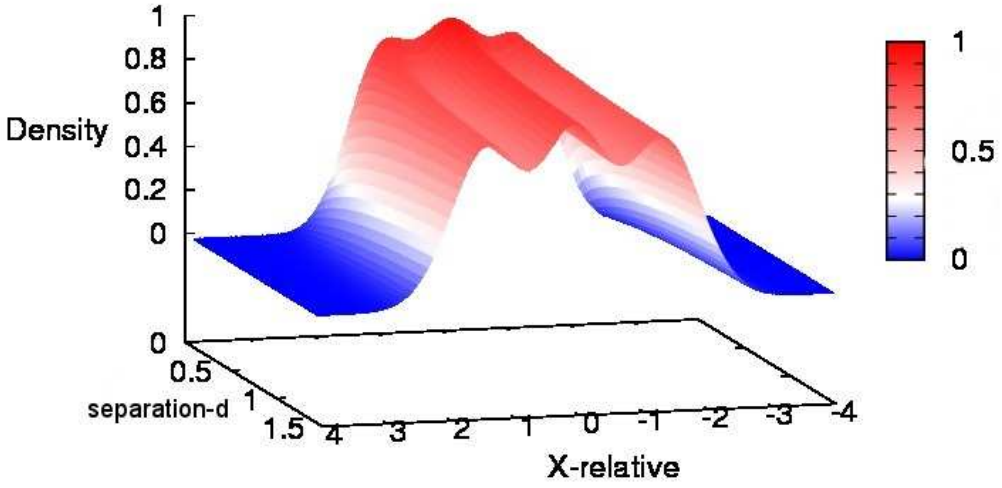

(a) $g = 1$

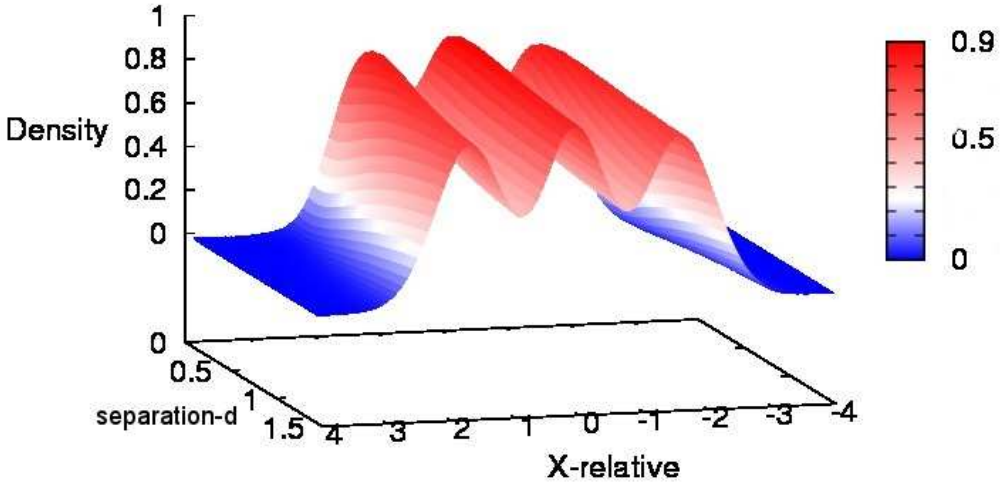

(b) $g = 3$

Figure C.2: $N = 6$ bosons in a double trap by sweeping d from 0.1 to 1.5.

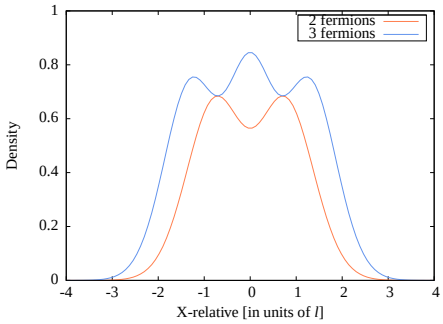

(a) $g = 0$

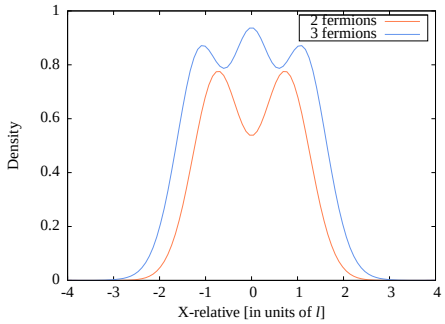

(b) $g = 2$

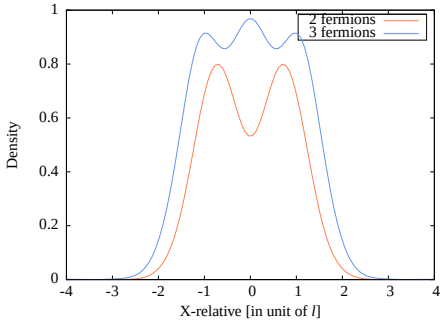

(c) $g = 4$

Figure C.3: Comparison of electron-hole systems for 2 and 3 particles at $d = 0.2$.

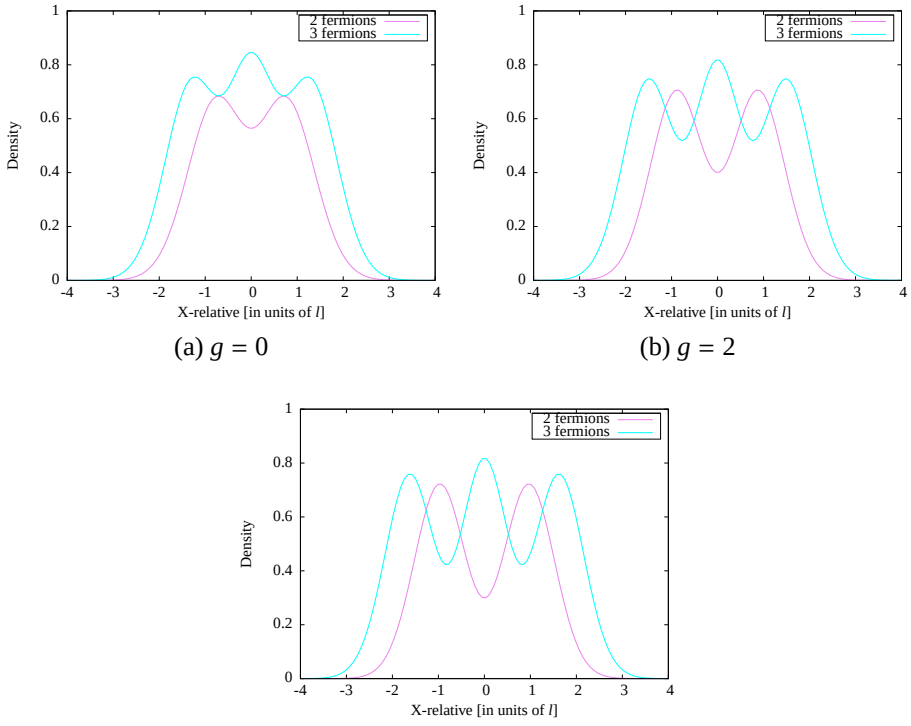

(a) $g = 0$ (b) $g = 2$

(c) $g = 4$

Figure C.4: Comparison of electron-hole systems for 2 and 3 particles at $d = 1$.

Fig. C.3 and Fig. C.4 show the behaviour of a system with non-perpendicular electron and hole pairs, since the particles in the two traps are not equal. In this case, I did not carefully check the convergence problem, but in principle the result can be trusted because the total number of particle is 5 (which should be easier to get to converge than with 6 particles).

Acknowledgements

I am most grateful to my supervisor, Professor Stephanie Reimann for providing me with such an interesting project and her perceptive insight. Many thanks go to Lìney for her kind guidance and patient explanations. Also it is a pleasure to thank Professor Cecilia Jarlskog for a careful reading of the manuscript and her many valuable comments. Not only did she help me to improve my English writing skills, but she let me know how important it is to have curiosity, enthusiasm and passion in my own work. Besides I would like to thank all the members in Steffi's group and everyone at the matfys division, for their open minds and delightful conversations. Finally, my special thanks go to a musician I have met here. Thanks to him for the first time I truly appreciate the beauty of classical music. Last but not least I wish to thank all my friends and my family for their invaluable help and support.

Bibliography

[1] J. Frenkel, “On the transformation of light into heat in solid”, Phys. Rev. 37:17-44, (1931).

[2] Gregory H. Wannier, “The structure of electronic excitation levels in insulating crystals”,Phys. Rev. 52:191-197, (1937).

[3] John M. Blatt, K. W. Böer, and Brandt Werner, “Bose-einstein condensation of excitons”, Phys. Rev. 126: 1691-1692, (1962).

[4] D. W. Snoke, “Coherence and optical emission from bilayer exciton condensates”, Condensed Matter Physics, (2011), 938609.

[5] L. H. Kristinsdóttir, Master thesis, *“The role of inter-species interaction strength in a two component rotating boson gas”*, Lund university, (2009).

[6] Harvey M. Deitel and Paul J. Deitel, *“C++ How to program”*, fifth edition, Pearson, (2005).

[7] Jonas C. Cremon, Ph.D thesis,*“Quantum few-body physics with the configuration interaction approach”*, Lund university, (2010).

[8] F. Deuretzbacher, Jonas C. Cremon and S. M. Reimann, “Ground-state properties of few dipolar bosons in a quasi-one-dimensional harmonic trap”, Phys. Rev. A, 81:063616, (2010).

[9] Jonas C. Cremon, G. M. Bruun and S. M. Reimann, “Tunable Wigner states with dipolar atoms and molecules”, Phys. Rev. 105:255301, (2010).

[10] D. W. Snoke, “Coherent exciton waves”, Science, 273:1351, (1996).

[11] Johannes Bjerlin, Master-thesis *“Dipole-dipole interaction in quasi one-dimensional harmonic traps”*, Lund university, (2012).

[12] Justin B. Sambur, Thomas Novet and B. A. Parkinson, “Multiple exciton collection in a sensitized Photovoltaic system”, Science, 330:1191462, (2010).

[13] M. H. G. de Miranda, A. Chotia, B. Neyenhuis, D. Wang, G. Quéméner, S. Ospelkaus, J. L. Bohn, J. Ye and D. S. Jin, "Controlling the quantum stereodynamics of ultracold bimolecular reactions", Nature physics, 7,6:502-507, (2011).

[14] Alexander L. Fetter and John D. Walecka *"Quantum theory of many-particle systems"*, Dover, (1971) edition.

[15] E. Poem, Y. Kodriano, C. Tradonsky, N. H. Lindner, B. D. Gerardot, P. M. Petroff and D. Gershoni, "Accessing the dark exciton with light", Nature physics, 6,12:993-997, (2010).

[16] Belén Paredes, Artur Widera, Valentin Murg, Olaf Mandel, Simon Fölling, Ignacio Cirac, Gora V. Shlyapnikov, Theodor W. Hänsch and Immanuel Bloch, "Tonks-Girardeau gas of ultracold atoms in an optical lattice", Nature, 429:277-281, (2004).

[17] Zoltán Vörös and D. W. Snoke, "Quantum well excitons at low density", Modern physics letters B, Vol.22, No.10(2008) 701-725.

[18] L. V. Butov, "Cold exciton gases in coupled quantum well structures", J.phys.:Condens. Matter 19(2007) 295202.

[19] M. H. Anderson, J. R. Ensher, M. R. Matthews, C. E. Wieman and E. A. Cornell, "Observation of Bose-Einstein condensation in a dilute atomic vapor", Science, 269(5211):198-201 (1995).

[20] C. C. Bradley, C. A. Sackett, J. J. Tollett and R. G. Hulet, "Evidence of Bose-Einstein condensation in an atomic gas with attractive interactions", Phys. Rev. Lett., 75(9):1687-1690, (1995).

[21] K. B. Davis, M. O. Mewes, M. R. Andrews, N. J. van Druten, D. S. Durfee, D. M. Kurn and W. Ketterle, "Bose-Einstein condensation in a gas of sodium atoms. Phys. Rev. Lett., 75(22):3969-3973, (1995).

[22] M. Girardeau, "Relationship between systems of impenetrable bosons and fermions in one dimension", J.Math.Phys. 1, 516-523, (1960).

[23] E. H. Lieb and W. Liniger, "Exact analysis of an interacting Bose gas. The general solution and the ground state", Phys. Rev. 130, 1605-1616, (1963).